

Study of the 2012 lahar on Iztaccíhuatl Volcano (Central Mexico) based on geomorphology, botanical evidence and 2D modeling

Estudio del lahar de 2012 en el volcán Iztaccíhuatl (México central) a partir de geomorfología, evidencia botánica y modelación 2D

José Ernesto **Figueroa-García**^{1,*}, Osvaldo **Franco-Ramos**², Lizeth **Caballero**³,
Juan Antonio **Ballesteros-Cánovas**⁴, José María **Bodoque**⁵

¹ Posgrado en Geografía, Universidad Nacional Autónoma de México. Ciudad Universitaria, 04510, Coyoacán, Ciudad de México, México.

² Instituto de Geografía, Universidad Nacional Autónoma de México. Ciudad Universitaria, 04510, Coyoacán, Ciudad de México, México.

³ Escuela Nacional de Ciencias de la Tierra, ENCiT. Universidad Nacional Autónoma de México. Ciudad Universitaria, 04510, Coyoacán, Ciudad de México, México.

⁴ National Museum of Natural Sciences, Spanish Research Council, MNCN-CSIC, C/ Serrano 115bis, 28006, Madrid, Spain.

⁵ Department of Mining and Geological Engineering, University of Castilla-La Mancha. Av. Carlos III s/n, 45071, Toledo, Spain.

* Corresponding author:
J.E. Figueroa-García ernestfigue.7@gmail.com

How to cite this article:

Figueroa-García, J.E., Franco-Ramos, O., Caballero, L., Ballesteros-Cánovas, J.A., Bodoque, J.M., 2025, Study of the 2012 lahar on Iztaccíhuatl Volcano (Central Mexico) based on geomorphology, botanical evidence and 2D modeling: Boletín de la Sociedad Geológica Mexicana, 77(3), A300625. <http://dx.doi.org/10.18268/BSGM2025v77n3a300625>

Manuscript received: March 10, 2025

Corrected manuscript received: June 24, 2025

Manuscript accepted: June 27, 2025

Peer Reviewing under the responsibility of Universidad Nacional Autónoma de México.

This is an open access article under the CC BY-NC-ND license (<https://creativecommons.org/licenses/by-nc-nd/4.0/>)

ABSTRACT

Lahars are high-energy surface processes capable of drastically transforming landscapes as they move downhill. These events often pose significant risks to populations living in volcanic mountain regions worldwide. Understanding the triggering mechanisms and spatio-temporal flow dynamics of lahars is crucial for anticipating their impacts. Although this geomorphological process has been analyzed in a number of volcanic areas, there are still regions where data concerning its triggers and behavior during its development is lacking. In this study, we applied a retrospective approach using field assessments, dendrogeomorphological methods, and numerical simulations to analyze a lahar event that occurred in the Alcalicán Valley of the Iztaccíhuatl volcano (Mexico). Scars on existing pine trees (*Pinus hartwegii* sp.) served as benchmarks to estimate the event's discharge as well as their spatial extent, using the open-source software HEC-RAS. Additionally, a thorough review of meteorological data was conducted to ascertain the probable triggering mechanisms of the event. The findings of this study suggest that the 2012 lahar event was triggered by rainfall associated with the impact of Hurricane Ernesto, which occurred between August 1st and 10th, 2012. During this period, a total of 230 mm of accumulated rainfall was recorded, with a maximum of 48 mm in a 24-hour period on August 5th. The maximum runout distance was estimated to be 750 m from the point at which the main channel begins to exhibit a single course, with a peak discharge rate of 5 m³/s. The lahar's maximum flow thickness reached 3 m, resulting in an estimated total volume of 3x10⁴ m³. Our analysis provides valuable baseline data for developing risk management strategies for the Iztaccíhuatl-Popocatepetl National Park. Furthermore, our findings demonstrate the added value of integrating multiple techniques to retrospectively gather information on past lahar events worldwide.

Keywords: lahar, Iztaccíhuatl Volcano, dendrogeomorphology, Paleo stage indicators, numerical modelling

RESUMEN

Los lahares son procesos superficiales de alta energía capaces de transformar drásticamente los paisajes a medida que se desplazan ladera abajo. Estos fenómenos suelen presentar riesgos importantes para las poblaciones que viven en regiones montañosas de carácter volcánico en todo el mundo. Comprender los mecanismos desencadenantes y la dinámica espaciotemporal de los lahares es crucial para anticipar sus impactos. Aunque este proceso geomorfológico se ha analizado en varias zonas volcánicas, todavía hay regiones en las que faltan datos sobre sus desencadenantes y su comportamiento durante su desarrollo. En este estudio, aplicamos un enfoque retrospectivo utilizando evaluaciones de campo, métodos dendrogeomorfológicos y simulaciones numéricas para analizar un evento de lahar que ocurrió en el Valle Alcalicán del volcán Iztaccíhuatl (México). Las cicatrices en los pinos existentes (*Pinus hartwegii* sp.) sirvieron como puntos de referencia para estimar la descarga del evento, así como su extensión espacial, utilizando el software de código abierto HEC-RAS. Además, se llevó a cabo una revisión exhaustiva de los datos meteorológicos para determinar los probables mecanismos desencadenantes del fenómeno. Los resultados de este estudio sugieren que el evento de lahar de 2012 fue desencadenado por las lluvias asociadas con el impacto del huracán Ernesto, que se produjo entre el 1 y el 10 de agosto de 2012. Durante este período, se registró un total de 230 mm de precipitación acumulada, con un máximo de 48 mm en un período de 24 horas el 5 de agosto. La distancia máxima de escurrimiento se estimó en 750 m desde el punto en el que el canal principal comienza a mostrar un único cauce, con una descarga máxima de 5 m³/s. El espesor máximo del lahar alcanzó los 3 m, dando lugar a un volumen total estimado de 3x10⁴ m³. Nuestro análisis proporciona datos de referencia valiosos para desarrollar estrategias de gestión de riesgos para el Parque Nacional Iztaccíhuatl-Popocatepetl. Además, nuestros resultados demuestran el valor añadido de integrar múltiples técnicas para recopilar retrospectivamente información sobre lahares ocurridos en el pasado en todo el mundo.

Palabras clave: lahar, volcán Iztaccíhuatl, dendrogeomorfología, Paleo indicadores de nivel, modelado numérico

1. Introduction

In volcanic environments, lahars are among the most common geomorphological processes. These flows are characterized by a mixture of sediments and water that move through the channels forming part of the mountain system at high velocities favored by the steep slopes (Wohl and Scott, 2017). Lahars can be triggered by several factors, including torrential rainfall associated to hurricanes (Quesada-Román *et al.*, 2019; Thouret *et al.*, 2020; Figueroa-García *et al.*, 2021), the melting of snow or glaciers (Pierson *et al.*, 2014; Pistolesi *et al.*, 2014; Delgado-Granados *et al.*, 2015), water saturation in sediments and soil pores (Baumann *et al.*, 2020; Tayyebi *et al.*, 2022), and seismic activity such as earthquakes (Coviello *et al.*, 2021; Arroyo-Solórzano *et al.*, 2022).

Lahars can be classified based on the timing of their occurrence. Those that occur simultaneously with volcanic activity are termed syn-eruptive lahars. In contrast, lahars generated shortly after an eruption, consisting of freshly deposited materials, are referred to as post-eruptive lahars (Manville *et al.*, 2009; Capra *et al.*, 2018). Lastly, lahars that take place during periods of volcanic quiescence are known as intra-eruptive lahars (Saucedo *et al.*, 2008). It is the latter two types (intra and post-eruptive) that are most frequently triggered by extreme hydrometeorological processes events (Worni *et al.*, 2012).

The study of lahars has become increasingly important due to the significant disruption they cause to inhabited volcanic areas. The damage they inflict can range from socio-economic and infrastructure issues, to the loss of human lives (Pierson *et al.*, 2014). Consequently, the main objective of understanding the spatial and temporal characteristics of these phenomena, is to devise strategies aiming at disaster risk reduction (Wilford *et al.*, 2009). However, a major challenge in assessing the potential risk of lahars is the lack of comprehensive data, especially in high mountainous regions that are often inadequately monitored. The available information is typically

limited to qualitative observations and reports from residents living near these sites.

Dendrogeomorphological methods have emerged as a valuable approach for studying the frequency and magnitude of lahars (Bollschweiler *et al.*, 2010; Salaorni *et al.*, 2017; Bovi *et al.*, 2022; Quesada-Román *et al.*, 2022). By examining the effects of lahars on trees in the vicinity of the streams where they occur, it is possible to accurately date the events, determine their spatial distribution and, once the geomorphological processes have been dated, establish the respective correlations with possible triggers (Tichavský, 2023). The disturbances recorded in the tree rings allow the determination of annual chronologies and can even achieve seasonal resolution, offering valuable insights into the investigated lahar processes (Stoffel and Corona, 2014).

To gain a deeper understanding of lahar transport and emplacement, several works have employed numerical models to reconstruct flood areas, flow depths, and velocities. While this approach represents an important development in the understanding of the processes, there is often a degree of uncertainty in model calibration and validation due to the scarcity of data, such as values for maximum peak discharge, flow duration, sediment content, and other critical parameters. One methodology that has been proposed in recent years to address these absences is the use of Paleo Stage Indicators or PSI (Benito and Thorndycraft, 2005; Baker, 2008; Bodoque *et al.*, 2011). PSI have a geomorphological origin and are typically represented by deposits, residual material, eroded channels, interrupted alluvial fans, and mud scarps (Bodoque *et al.*, 2011). Additionally, botanical indicators, such as those utilized in this research, allow PSIs to serve not only as markers of maximum flood levels, but also as tools for visualizing flood recurrence over time. The key advantage of using PSIs is that they help reduce uncertainty in determining the frequency of lahar flows over periods ranging from hundreds to thousands of years (Bodoque *et al.*, 2015).

The trees affected by the flow in torrential systems can be considered to be markers of the maximum height of the phenomenon (PSI) (Ballesteros Cánovas *et al.*, 2011; Díez-Herrero *et al.*, 2013; Ballesteros-Cánovas *et al.*, 2015a, 2015b; Ballesteros-Cánovas *et al.*, 2016). PSIs were initially applied to reconstruct torrential floods in mountainous environments in Europe (Ruiz-Villanueva *et al.*, 2010; Ballesteros-Cánovas *et al.*, 2015a, 2015b; Ballesteros-Cánovas *et al.*, 2016), in tropical areas (Quesada-Román, 2023; Quesada-Román, 2024; De la Peña Guillen *et al.*, 2025), and their effectiveness in lahar reconstruction and magnitude estimation was corroborated in Mexican volcanic areas (Franco-Ramos *et al.*, 2013, 2016a, 2016b, 2017, 2020; Figueroa-García *et al.*, 2021). Despite these advancements, significant uncertainties persist regarding the calculation of lahar discharge and the energy of debris flows in quiescence volcanic regions, which demands further investigation.

Over the past three decades, numerical modelling has been employed extensively to study geomorphological processes, including floods (Brunner *et al.*, 2021), landslides (Boyd *et al.*, 2021) and debris flows (Schraml *et al.*, 2015). This approach has significantly enhanced our understanding of the physical behavior of these phenomena, allowing for the realistic reconstruction of volumes, velocities, spatial distributions, and the development of potential future scenarios. Lahar modelling has been a crucial aspect of many studies (Castruccio and Clavero, 2015; Caballero *et al.*, 2016; Frimberger *et al.*, 2021; Procter *et al.*, 2021), with efforts directed towards replicating past events, deciphering the internal dynamics of flows, and mapping spatial distributions to identify potential impact zones. The most widely used software for lahar modeling includes LAHARZ (Schilling, 2014), Titan 2D (Williams *et al.*, 2008), FLO2D (O'Brien *et al.*, 1993) and RAMMS (Bühler *et al.*, 2011; Christen *et al.*, 2012). However, in this research, we propose the use of the open-source HEC-RAS 6.2 software, developed by the U.S.

Army Hydrologic Engineering Center (Brunner, 2002). This software allows for the modelling of one-dimensional steady flow, one-dimensional and two-dimensional unsteady flow, sediment transport/moving bed calculations, and water temperature/water quality. The latest update, the DebrisLib module, incorporates the modelling of mud and debris flows (Gibson *et al.*, 2021; Gibson *et al.*, 2022). Although HEC-RAS has been used sparingly to replicate debris flows and lahars (Gibson *et al.*, 2022; Pandey *et al.*, 2022; Yilmaz *et al.*, 2023), it offers certain advantages over other simulators. These include the ability to model different equations based on the type of flow, options to adjust viscosity and yield stress values, a logical and straightforward sequence of operations, and, importantly, its status as an open-source program.

The aims of this study are to reconstruct the 2012 lahar in the Alcala Valley (Iztaccihuatl, Central Mexico) using dendrogeomorphological methods (paleo stage indicators) and to simulate it numerically with the open-source software HEC-RAS 6.2. Specifically, we analyze tree rings affected by the lahar to establish the spatial and temporal characteristics of the event, with the purpose to accurately determine the date and extent of the lahar. Additionally, we aim to demonstrate the effectiveness of HEC-RAS in simulating lahars in high-altitude volcanic regions. Another key aspect of this research is the identification of the hydrometeorological factors that triggered the 2012 lahar event.

2. Study area

The study area corresponds to the Iztaccihuatl volcanic complex (Iztaccihuatl-Popocatepetl National Park), which is part of the Sierra Nevada volcanic mountain range (Figure 1A), located in the central-eastern portion of the Trans-Mexican Volcanic Belt (TMVB; Nixon, 1989). It is important to highlight the morphological characteristics of the Iztaccihuatl

volcanic complex, which encompasses proximal volcanoclastic deposits, domes, and lava flows that have been dated between 0.9 and 0.6 Ma, spread over a total length of 7 km with a N-S orientation (Nixon, 1989) (Figure 1B). Although the structure has several volcanic formations, the most interesting (due to the location of the study area), is the volcano known as Los Pies, which is characterized by its formation in two periods, defined as: the Ancient Los Pies cone, and the Recent Los Pies cone. Both cones are composed of dacitic and andesitic rocks (Macías *et al.*, 2012). The Recent Los Pies edifice has been dated around 0.41-0.34 Ma (Nixon, 1989) and its summit zone is characterized by an interbedding of lava flows and autoclastic breccias, with areas exhibiting intense hydrothermal alteration and

a moraine cover (Macías *et al.*, 2012; Figure 1C). A lateral collapse took place at 631 ± 44 ka (Sunyé-Puchol *et al.*, 2022) resulting in the formation of a truncated cone morphology with a horseshoe-shaped crater opening towards the SE. This collapse is represented by a debris avalanche deposit observed to the southeast of the Iztaccíhuatl volcanic complex (Macías *et al.*, 2012).

Another significant process in the study area, which still has ongoing implications to this day, is the glacial advance and retreat that occurred in different episodes in central Mexico. For example, Vázquez-Selem and Heine (2011), have identified the various glacial advances on the slopes of the Iztaccíhuatl volcanic complex, which have resulted in the formation of different morphologies, including moraines and glacial valleys.

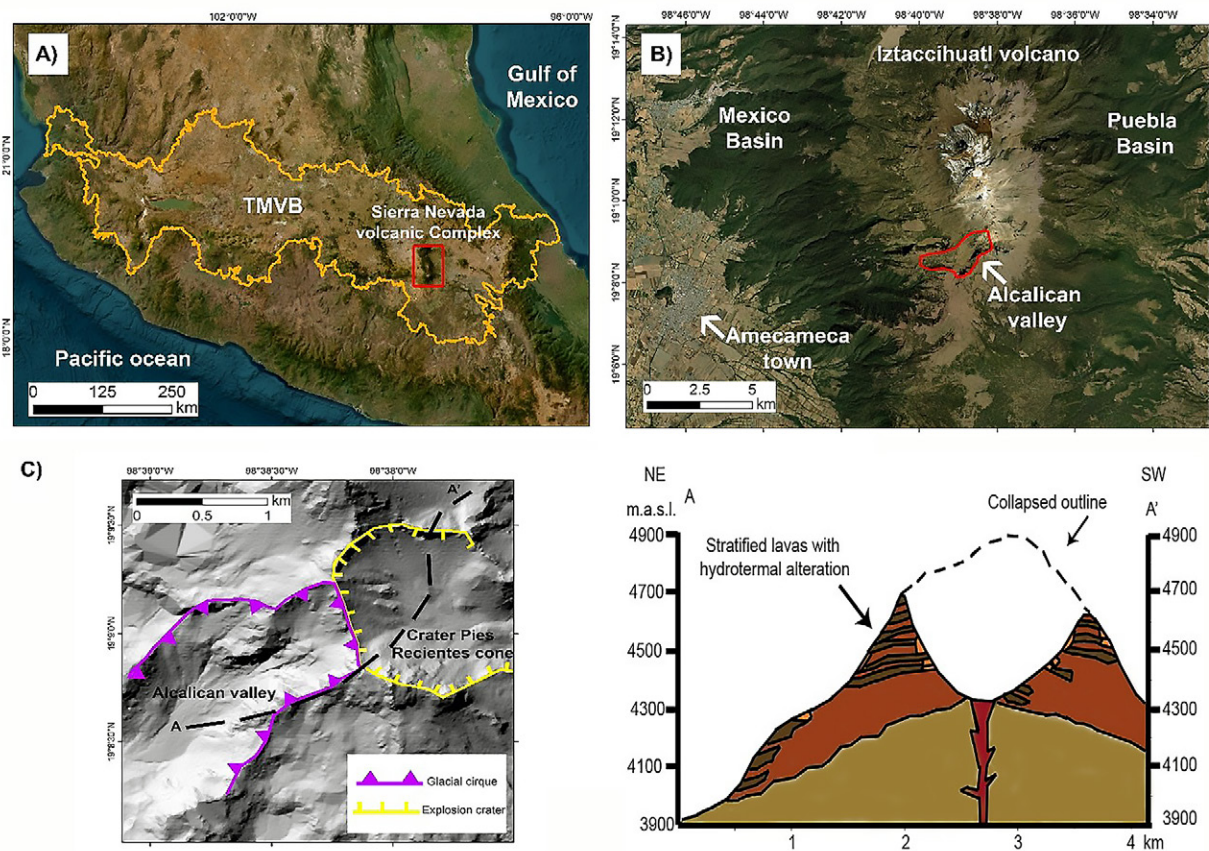


Figure 1 A) Regional localization of the study site in the central east of TMVB; B) The Iztaccíhuatl volcanic complex and the location of the Alcalican Valley in the southwestern portion of the recent Los Pies volcano. C) Geological and geomorphological profile illustrating the lithological conditions of the recent Los Pies volcano, where the Alcalican Valley is located. It shows that the upper portion of the valley is formed by a sequence of lavas fractured by volcanic, glacial, and periglacial activity (Modified from Macías *et al.*, 2012).

One of these glacial valleys is the Alcalican Valley, where the lahar event studied here took place in 2012. This valley is located on the southwestern sector of the Iztaccíhuatl volcanic complex, between the following coordinates: 19°8.735' N; 98°38.738' W (Figure 1B-C). It covers an area of approximately 4 km², with a length of 3.03 km and an average width of 1.07 km, reaching a maximum width of 1.43 km. The catchment elevation range is 656 m with a maximum elevation of 4 533 m a.s.l. The average channel slope is 28°.

Another noteworthy feature of the Alcalican Valley is its history of glacial advances, which is evident in its U-shaped profile with a flat bottom. Furthermore, evidence of moraines and glacial polishing can be observed in the lateral sections of the valley, indicating the occurrence of the last advances corresponding to Milpulco 1 (Vázquez-Selem and Heine, 2011). Additionally, in the upper portions of the basin, there is a high degree of rock fracturing due to the glacial modelling that occurred in the Pleistocene, and the current conditions of glacial weathering (*e.g.*, gelifraction), which generates conspicuous rock falls towards the valley.

The biophysical features of the Alcalican Valley include the presence of regosols and cambisols (CONANP, 2013). In addition, López-López *et al.* (2023) include the vitric andosol between 3 000 to 4 300 m a.s.l., which is associated with the formation and deposition of volcanic materials younger than 1 100 yr. The most active geomorphic processes (sheet erosion), occurred on the south-facing slope due to increased solar radiation and higher fire frequency (López-López *et al.*, 2023). Sheet erosion can be intensified between 3 500 and 4 500 m a.s.l. This is due to the mean annual ground temperature (0° to 3°C) and periglacial processes, which are more active at this altitude (Andrés *et al.*, 2011). Furthermore, the mean annual precipitation is 750 mm, with the months of June to September exhibiting the highest rainfall and a monthly average of 160 mm, while the driest months occur during the winter (CONANP, 2013). The dominant vegetation in the valley is grassland (*Festuca* sp.) and *Pinus hartwegii* trees (CONANP, 2013).

Therefore, when considering the historical and current state of the Iztaccíhuatl volcano, it becomes evident that the Alcalican valley is subject to ongoing surface geomorphological processes. These dynamics are primarily driven by water runoff and gravitational processes, which continually reshape the surface of the valley and result in notable, and sometimes abrupt, morphological modifications to the valley's channels.

3. Materials and methods

3.1. UAV PHOTOGRAMMETRY AND GEOSPATIAL DATA COLLECTION

During the fieldwork (April 2022), we conducted photogrammetric flights using a UAV to obtain a detailed topography of the work area. Two aspects were considered when selecting the modeling area. First, the absence of tributary flows indicated that the lahar had fully developed in a single channel, thus the integration of water with sediments from other areas would not affect the simulation. Second, the simulation zone needed to be characterized by a slope that favoured sedimentation over erosion. This consideration was important because the model has volume conservation characteristics.

Specifically, we used a DJI Mavic 2 Pro drone flying at an altitude of 60 m above the surface. To ensure comprehensive coverage, we maintained an 80% overlap between photographs. Once this was corroborated, the project was generated using the Pix4Dcapture App. To achieve a highly accurate model, we collected a series of points with a millimetric GNSS/GPS system (Emild Rs + and the Reach View app). For this purpose, 1x1-meter tarps were placed in different areas of the valley to ensure visibility in the photographs taken by the drone, and a total of 5 points were acquired for model correction. It is essential to highlight that the points obtained were recorded under the Fix solution, meaning that the accuracy of the points was within centimeters, due to the correction provided by the rover from the

base station. Moreover, we made observations of the deposits associated with the lahar flow, as well as the landforms related to this process. We identified levees, lobes of material within the main channel, and blocks that impacted trees. To further validate the generated DEM for modeling, eight profiles were created using the millimetric GNSS/GPS. These profiles were used to compare the shape of the channel and identify any obstacles that could potentially introduce errors in the modeled discharge. Furthermore, 18 measurements of the deposit's thickness were taken across the entire inundated area to determine the average volume of the lahar. The resulting values were then averaged and subsequently multiplied by the total area of the lahar.

3.2. PHOTOGRAMMETRIC PROCESSING AND GEOMORPHOLOGICAL MAPPING OF LAHAR DEPOSITS

In the laboratory, we used Pix4Dmapper software (Pix4D SA, Switzerland) to perform photogrammetric processing of the UAV flights. This software utilizes Structure from Motion (SfM) techniques. A total of 703 photographs were processed, all of which had accurate geolocation in the WGS84 UTM Zone 14 coordinate system. Additionally, points obtained with the millimetric GPS were integrated into the program, resulting in different outputs (*i.e.* orthomosaic and digital surface models). The vegetation was filtered from the point classification methods included in Pix4Dmapper. The final resolution of the DEM was 70x70 cm/pixel with an error of 2 cm in all axes (x, y, z).

To characterize the lahar deposit, geomorphological mapping of the study area was carried out at two distinct scales. For the regional scale map, the DEM with a 15 m resolution, provided by INEGI (National Institute of Statistics and Geography), was used in conjunction with satellite images from Google Earth™ to contextualize the entire valley. Detailed mapping was performed using both the

DEM and the orthomosaic generated during the UAV flight, allowing for the delineation of the landforms associated with the 2012 lahar deposit. Georeferencing and mapping were conducted using ArcGIS 10.8.

3.3. DENDROGEOMORPHOLOGICAL CHARACTERIZATION

To reconstruct the magnitude of the lahar, we used techniques from dendrochronology and paleohydrology. The dendrogeomorphological analysis was conducted on six *Pinus hartwegii* sp. trees that were impacted by the lahar, from which a total of 13 cores were obtained. These trees were strategically located near the main channel of the Alcalican Valley, making them ideal for geomorphological analysis. It is important to note that all trees in the area exhibiting evidence of impact were included in the sampling. The low number of collected trees is attributed to the site's proximity to the tree line. These trees were identified as PSI, and data were collected from them, including the maximum debarking height, millimetric GNSS/GPS system, and a reference measurement related to a visible relief element in the orthomosaic generated by the UAV (Benito and Thorndycraft, 2005; Ballesteros-Cánovas *et al.*, 2011; Bodoque *et al.*, 2015). This ensured accurate positioning during the modeling process (Figure 2). The samples from the all collected trees were processed and analyzed according to the dendrogeomorphological principles outlined by Stoffel and Corona (2014). These procedures involved measuring and dating each of the samples from the affected trees. Additionally, to ensure the accuracy of the dating, the measurements were correlated with a reference chronology previously developed for the same area of Iztaccíhuatl. The utility of the tree rings lies in their ability to provide annual and sub-annual dating of the laharic event, model its thickness and distribution as its relations with potential triggering factors.

3.4. LAHAR MODELLING

For the paleohydrologic analysis, we used the latest version of the open-source software HEC-RAS 6.2, which includes a new module (DebrisLib) (Gibson *et al.*, 2021; Gibson *et al.*, 2022). This module allows for the modeling of fluvial processes characterized by high percentages of sediments throughout the implementation of various equations. We used the O'Brien quadratic model (O'Brien *et al.*, 1993), which considers stresses due to: cohesion, internal friction between sediment and fluid, turbulence, and inertial impact between particles. This quadratic model can be expressed as:

$$\tau_{MD} = \tau_y + \tau_v + \tau_d \quad (1)$$

$$\tau_v = \mu m \gamma \quad (2)$$

$$\tau_d = c_{Bd} \rho_s \lambda^2 d_s^2 \gamma \cdot^2 \quad (3)$$

where τ_{MD} is the mud and debris stress which includes all non-Newtonian stresses, τ_y is the yield stress, τ_v is the viscosity, μm is the value that indicates the viscosity is greater than the fluid

alone, τ_d is the dispersive stress, c_{Bd} is an empirical coefficient, ρ_s is the sediment particle density, d_s is the representative particle diameter, λ is the linear sediment concentration and γ is the unit weight of the fluid.

In addition, the model takes into account two rheological coefficients, α and β , which are related to the yield stress and viscosity of the lahar, obtained from empirical data by O'Brien and Julien (1988). The textural characteristics of the deposit, *e.g.* coarse clasts supported by a sand-sized matrix, indicate that the lahar was a debris flow (Iverson *et al.*, 2011; Thouret *et al.*, 2020). Based on this information, a volumetric concentration of 50% was set into the model. A 20-minute hydrograph was used, taking into account some data reported in other areas of central Mexico (Muñoz-Salinas *et al.*, 2009; Caballero and Capra, 2014; Caballero *et al.*, 2016). The time for the peak discharge was set at 10 minutes. Table 1 summarizes the values and aspects considered in the simulation.

Three simulations were conducted, with varying peak discharge from 3 m³/s to 10 m³/s. This modification aimed to identify the optimal

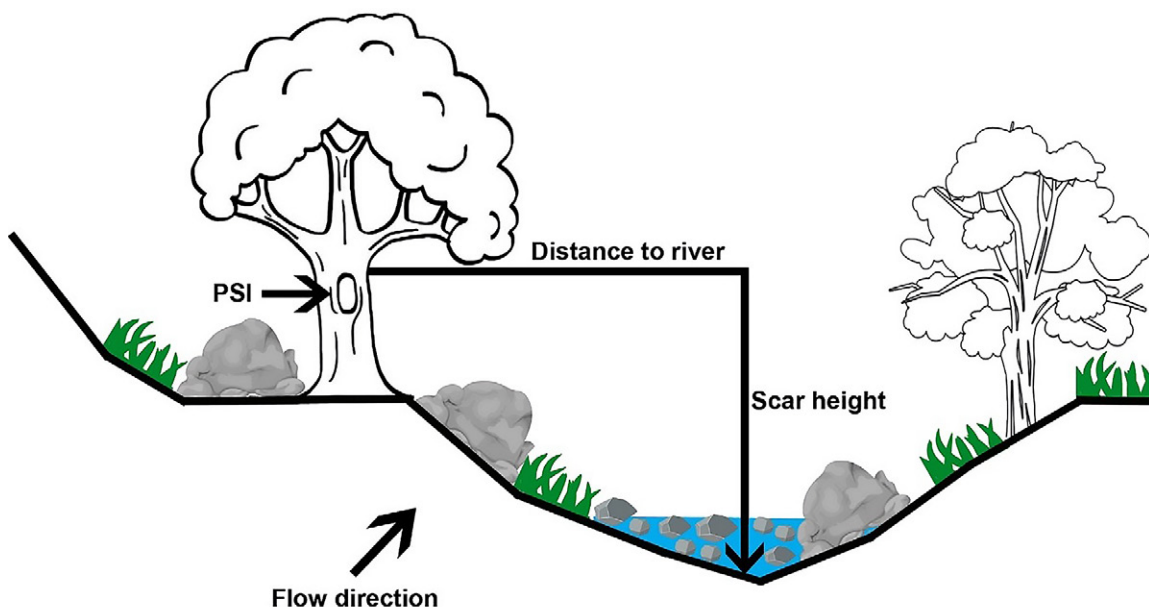


Figure 2 The diagram shows the elements to consider when collecting PSI data. It shows the identification of the scars generated by the lahar, which were measured for their maximum height in relation to the ground surface.

Table 1. Parameters used for the numerical simulation of the 2012 lahar in the Alcalican Valley using the HEC-RAS 6.2 program.

Parameters	Values
Modelled discharge peaks (m ³ /s)	3; 5; 10
Viscosity $\eta = \alpha e^{\beta C_v}$	$\alpha = 0.0648$ $\beta = 6.20$
Yield stress $\tau_y = \alpha e^{\beta C_v}$	$\alpha = 0.0765$ $\beta = 16.9$
Volumetric concentration	0.5
Modelling time	20 minutes
Time to peak discharge	10 minutes

match between the trees utilized as PSI and the depths observed in each simulation. To assess the compatibility between the maximum flow depth and the tree debarking, the difference between these two values was calculated, and an average of these differences was derived. Each result was then subjected to a linear regression to determine the value with the best statistical fit. Furthermore, the standard deviation of the differences obtained was calculated to ascertain which trees exhibited the optimum correlation between maximum scar height and maximum modelled depth.

3.5. SENSITIVITY ANALYSIS OF RHEOLOGICAL PARAMETERS AND MODEL VALIDATION UTILIZING GEOMORPHOLOGICAL DATA

Prior to defining the optimal modelling parameters, a sensitivity analysis was performed to evaluate the influence of the rheological coefficients on the lahar simulation results, ensuring that the selected parameters closely represent real-world conditions. The lahar distribution observed in satellite images a few months after the event (November, 2012), served as a benchmark for comparison. The simulations were structured as follows: one simulation reduced the viscosity and yield stress values to represent a less viscous lahar, while another increased these values to simulate a more viscous lahar. A third simulation decreased the volumetric concentration to 40%, while retaining the viscosity and yield stress values reported by O'Brien and Julien (1988) for Glenwood 2 (Table 2).

Quantitative validation of the simulated lahar was performed based on the percent length ratio (PLR) and the fitness function (e_1). Both comparisons were initially used by Proietti *et al.* (2009) to evaluate lava flows and were later applied to lahars by Caballero *et al.* (2016). The PLR compares flow runout and is defined as follows:

$$PLR = \frac{L_{sim}}{L_{obs}} \times 100 \tag{4}$$

where L_{sim} is the simulated length and L_{obs} is the observed length.

The second parameter, a fitness function named e_1 , was derived by Spataro *et al.* (2004) and compares the lateral spreading. It is defined as:

$$e_1 = \sqrt{\frac{m(R \cap S)}{m(R \cup S)}} \tag{5}$$

Where $R \cap S$ represents the overlapping area between the real flow and the simulation. $R \cup S$ indicates the sum of underestimated, overlapping, and overestimated areas between the observed event and simulations. A value of $e_1 = 1$ implies a perfect match between the real event and the simulation, and $e_1 = 0$ denotes a complete mismatch between them. For the calculation of variable e_1 , we used the same polygon generated during the geomorphological characterization, which corresponds to the spatial distribution of the 2012 lahar a few months after its occurrence.

Table 2 Parameters used to detect the sensitivity of rheological values in the HEC-RAS 6.2 program.

Simulation/Variable	Viscosity $\eta = \alpha e^{\beta C v}$	Yield stress $\tau_y = \alpha e^{\beta C v}$	Volumetric concentration	Discharge	Modelling time	Time of peak discharge
Less viscous lahar (S1)	$\alpha = 0.0486$ $\beta = 4.2$	$\alpha = 0.0465$ $\beta = 12.675$	50%	5 m ³ /s	20 min	10 min
More Viscous lahar (S2)	$\alpha = 0.081$ $\beta = 8.20$	$\alpha = 0.0965$ $\beta = 21.125$	50%	5 m ³ /s	20 min	10 min
Lahar with less volumetric concentration (S3)	$\alpha = 0.0648$ $\beta = 6.20$	$\alpha = 0.0765$ $\beta = 16.9$	40%	5 m ³ /s	20 min	10 min
2012 lahar (OS)	$\alpha = 0.0648$ $\beta = 6.20$	$\alpha = 0.0765$ $\beta = 16.9$	50%	5 m ³ /s	20 min	10 min

The polygon was generated on the raster of the simulation results obtained with the software HEC-RAS. This approach allowed us to clearly distinguish between surfaces with good overlap, and those that were over or underestimated. All of this was performed in ArcGIS 10.8.

In addition, to validate the peak discharge calculated by the model, the area of a channel cross-section was calculated by a trapezoidal shape at PSI number 3:

$$A = \frac{(B + b) \times h}{2} \tag{6}$$

where, *A* is the area of the trapezoid; *B* is the major base, equal to the upper portion of the channel (5 m); *b* is the minor base, equal to the horizontal distance of the channel (2 m); and *h* is the height, defined as the measurement provided by the PSI considered (1.10 m).

4. Results

4.1 GEOMORPHOLOGIC FEATURES OF THE 2012 LAHAR

The objective of the regional map (Figure 3A) is to provide an overview of the characteristics of the valley to identify the geomorphological sources of the laharic material. The Alcalican Valley is characterized by its glacial features, as evidenced by the well-defined cirque and the presence of

moraine deposits, indicating at least one maximum advance and several retreats (Milpulco I). Lava flows associated with the recent Los Pies period can also be observed. These lava flows are distinguished by a continuous detachment of material and generate active debris slopes on the northeastern slope of the valley. These features are the source of the material that originated the 2012 lahar.

The detailed map (Figure 3B) illustrates the geomorphic characteristics of the sector employed for numerical modelling. This view allows for a more accurate delineation of the landforms and flow distribution of the 2012 lahar. Furthermore, it identifies certain structures associated with old lahar lobes, providing evidence that the valley regularly experiences laharic dynamics under specific conditions. The detailed map also shows the location of the trees sampled for dendrogeomorphological analysis, placing them in their geomorphological context. Their proximity to the channel makes these trees optimal for the purpose of PSIs, as they are the only available specimens for calibration. The 2012 lahar inundated an area of 0.019 km², with a maximum runout of 750 m in a preferred NE-SW direction. The deposit features an average slope of 15°, an average thickness of 2.49 m, and an average volume of 3x10⁴ m³. The lahar flow filled the main channel, as evidenced by the presence of levees in the higher parts of the channel. At present, however, much of the sediment that once filled the

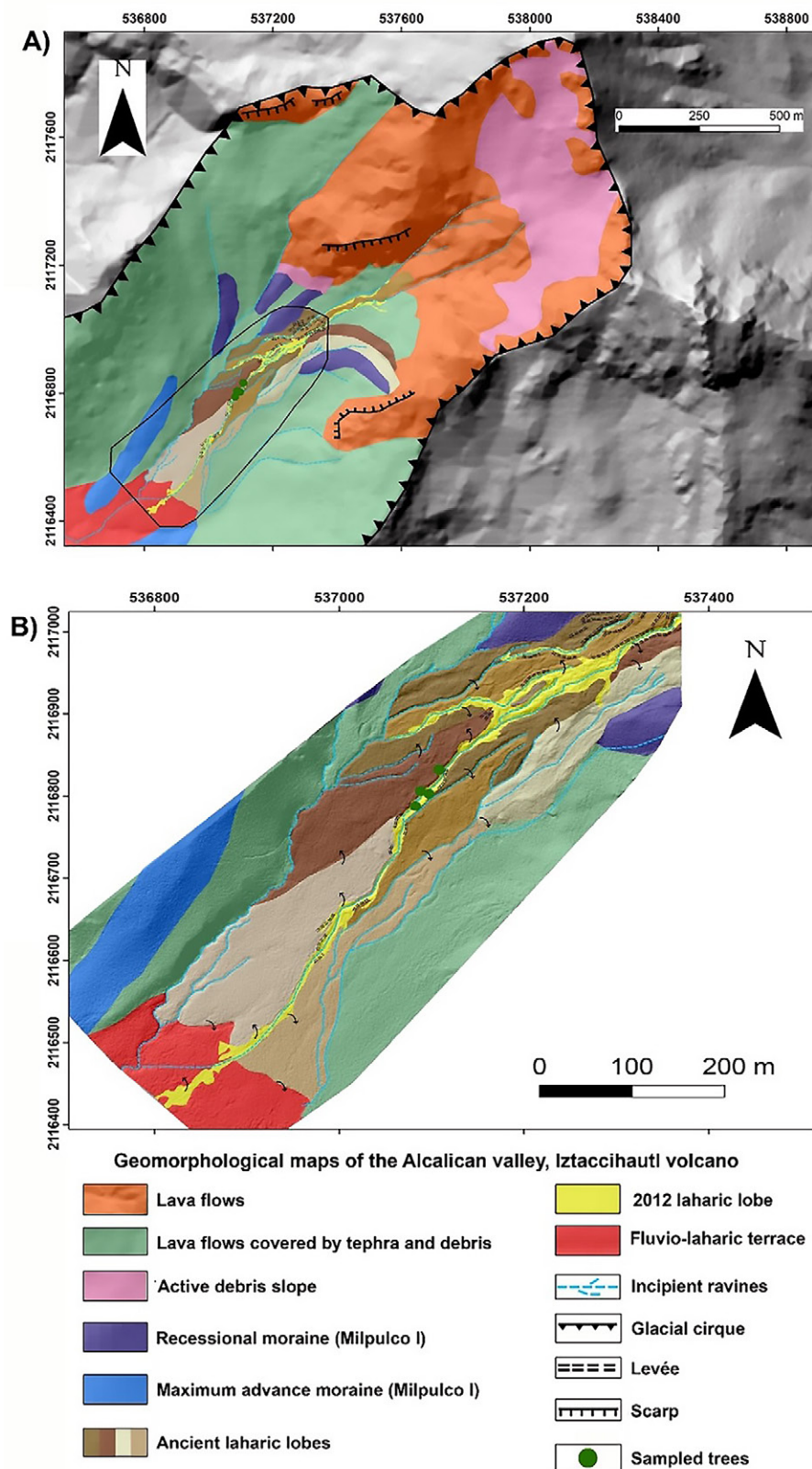


Figure 3 A) Geomorphological mapping of the general context of the Alcalican Valley. B) Geomorphological characterization of the study area conducted via photogrammetric flight using UAV and employed for numerical modelling of the lahar (WGS 84/UTM zone 14N).

channel has been remobilized, leaving only traces visible in the interior, and in the aforementioned levees. Another indicator of the flow's extent is the overflow of the main channel, which has led to the formation of secondary lobes.

The distribution of lahar deposits varies by location. Deposits near the flow source are characterized by coarseness, containing blocks and gravel (Figure 4A). In its distal section, the deposit shifts from coarser gravel to a finer mixture of sand and clay (Figure 4B). Notably, the deposit is ochre in color, making it easier to identify in satellite or UAV imagery. Finally, in the distal area, the deposit lies on a sub-horizontal surface, which is characterized by the continuous accumulation of fluvio-volcanic materials.

4.2 DENDROGEOMORPHOLOGY ANALYSIS AND TRIGGERS

The oldest *P. hartwegii* tree was 64 years old, while the youngest was 16. Scars related to the 2012 event were identified in 5 cores (45%), while compression wood from 2013 was observed in 6 cores (55%).

All injuries (Figure 5A-5B) were identified in the latewood, specifically at the end of this period, known as late-latewood. The sub-annual data provided by dendrogeomorphological methods allow for the identification of potential triggers within the specific period in which the impact is recorded. In this context, the latewood period extends from August to October for species found in Mexico. Therefore, upon examining rainfall data from meteorological stations near the study area, notable increases in precipitation were observed during the first 10 days of August 2012, coinciding with the impact of Hurricane Ernesto on central and southern Mexico (NOAA, 2019). At the Santiago Xalitzintla station, located 15 km from the study area, a total of 230 mm of accumulated rainfall was recorded between August 1st and 10th, with a maximum precipitation of 48 mm on August 5th. We chose this station because it was the closest one and provided the most accurate data. This suggests that, for the formation of some lahars, not only should intense single-day events be considered, but also accumulated rainfall may play a role in their development.

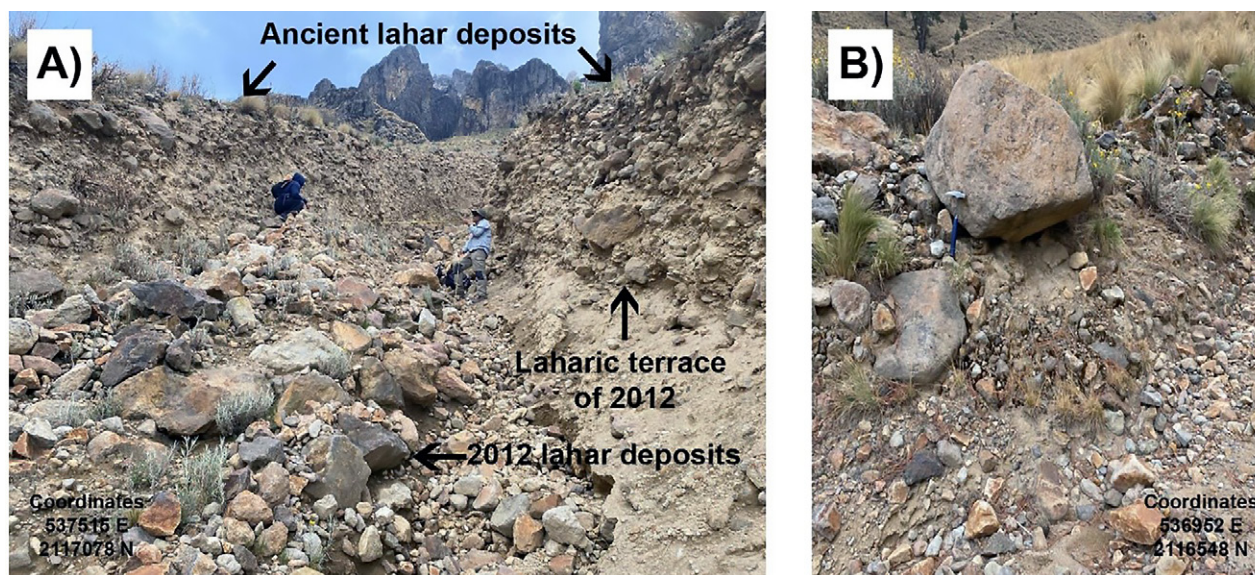


Figure 4 A) The proximal zone of the lahar deposit is characterized by a high concentration of blocks and gravel. The image illustrates deposits associated with older events that were not covered by the 2012 lahar, while the interior of the channel is filled with material associated with that event. B) In the middle and distal portions of the lahar, the deposited materials are characterized by gravel with some scattered blocks, along with a higher concentration of sands and clays that cement the materials associated with the flow.

4.3 NUMERICAL MODELING OF 2012 LAHAR

The results indicated a maximum discharge of $5 \text{ m}^3/\text{s}$, a flow depth of 2.78 m, and a maximum velocity of 2.5 m/s in the central channel (Figure 6A-B and 7A-B). Model validation was conducted using the PLR parameter for the distal reach of the deposit, the fitness function (e_f) for the area, and PSIs for flow depths. The PLR yielded a value of 107%, indicating that the distance reached by the simulated lahar was 7% greater (50 m) than the distance of the real flow. For function e_f , a value of 0.72 was obtained (Figure 8) with an overlapping area of 1.632 ha, an overestimated area of 1.161 ha, and an underestimated area of 0.303 ha. Regarding the PSIs, the trees used to validate the model results exhibited an average standard deviation of -0.01 m, with extreme values of -0.26 and 0.16 m.

The three validation approaches revealed that the most significant discrepancies were found in areas related to changes in the direction of the channel. These changes in the terrain were not accurately reflected in the simulated flows, resulting in the creation of additional areas of material deposition. This discrepancy is also responsible for the slight overestimation of the PLR.

Regarding the calibration of the peak discharge, the trapezoidal formula applied to the portion of the channel where PSI number 3 is located, yielded a result of 3.85 m^2 . This outcome requires a velocity of 1.3 m/s to mobilize a discharge of $5 \text{ m}^3/\text{s}$. This velocity value aligns with those shown on the velocity map generated by HEC-RAS (Figure 7B).



Figure 5 Increment cores with growth disturbances caused by the 2012 lahar. In both examples, some marks corresponding to the dating performed can be observed. In each case, these marks, from right to left, refer to the years 2010 and 2020, respectively. A) Compression wood that began to grow the year following the lahar event, specifically, in 2013. Its main characteristic is an increase in wood production, which usually appears as larger growth rings with a darker coloration. B) The injury was dated in the late-late wood of 2012.

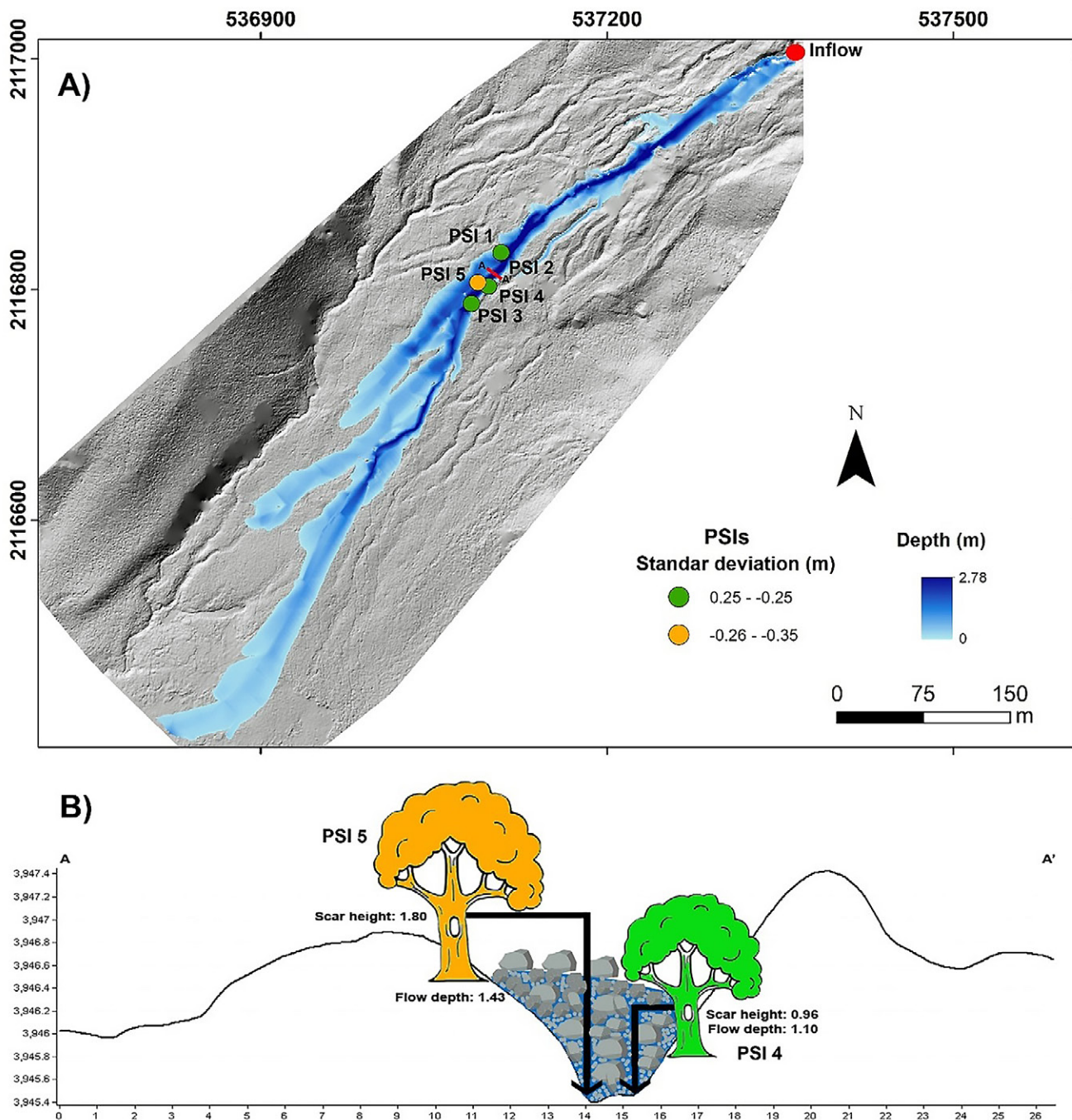


Figure 6 A) The 2012 lahar simulation in the Alcalican Valley using HEC-RAS. The green and orange dots show the position of the trees used as PSIs (WGS 84/UTM zone 14N). B) The profile displays the positions of the two trees identified as PSIs. The colors assigned to each tree correspond to their standard deviation values between the modeled and field measurements. The yellow tree presented a greater discrepancy between the PSI and flow depth, while the green tree demonstrated a better fit.

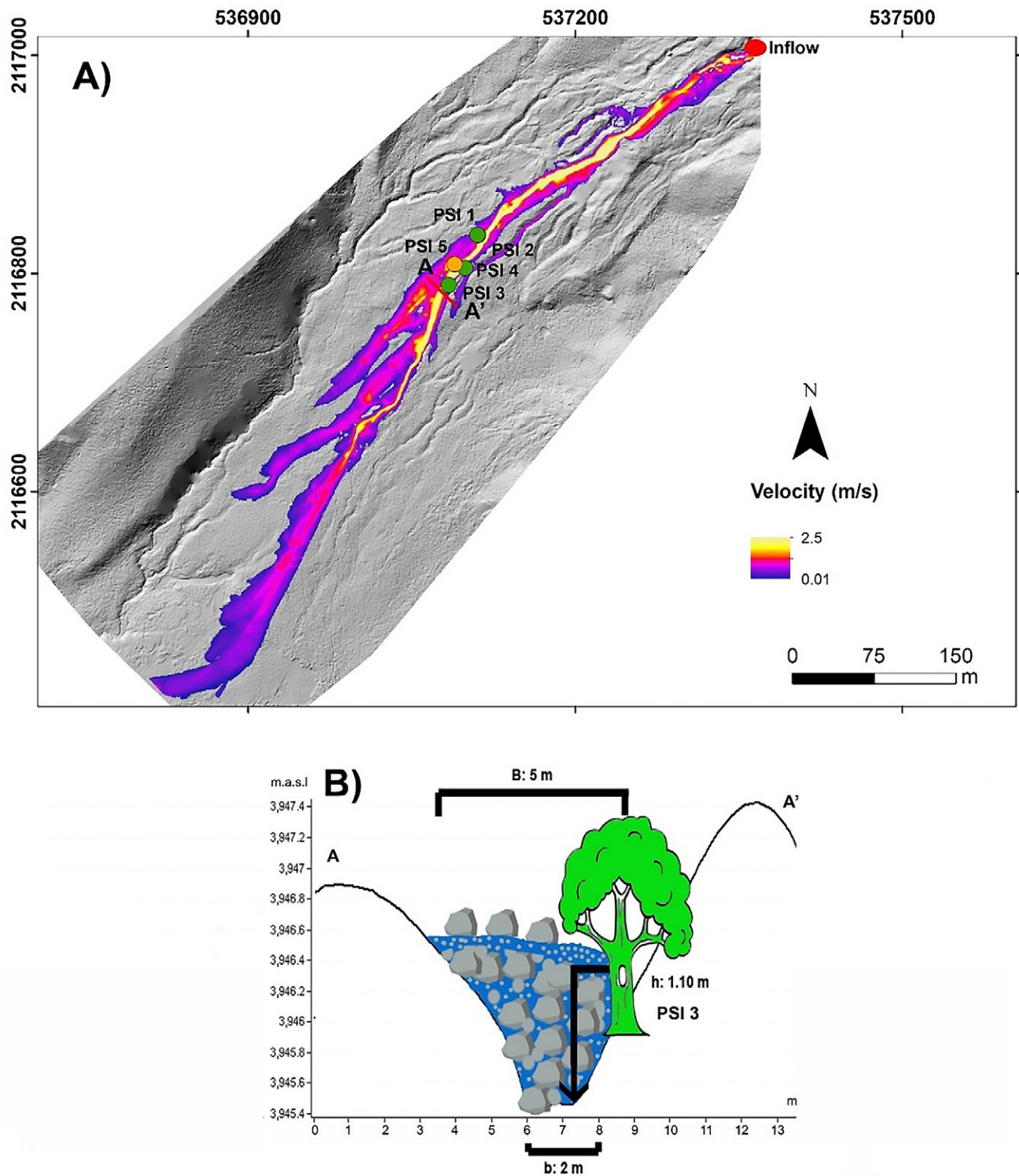


Figure 7 A) Numerical modelling with HEC-RAS allows us to recreate the velocity with which the lahar travelled through the main channel. Modelling outputs revealed that the central portion exhibited the highest velocity, reaching a maximum of 2.5 m/s. Once the lahar overflows, it loses its momentum and drastically reduces its velocity (WGS 84/UTM zone 14N). B) The diagram shows the measurements used to determine whether the discharge value obtained during modeling ($5\text{m}^3/\text{s}$) was realistic. For this purpose, it is assumed that the morphology of the channel is equivalent to a trapezoid, where B represents the major base, b the minor base and h the height of the debarking.

The sensitivity analysis (Figure 9A) revealed that, in the HEC-RAS software, variations in yield stress and viscosity have the greatest influence on the distribution and extent of the modeled lahars. In the simulation with a more dilute lahar (S1), areas of the valley that were not covered by the 2012 flow (as indicated by the black polygon) were included. Conversely, a more viscous lahar leads to a more constrained path, resulting in no overflow in other parts of the valley (S2). The simulation in which only the volumetric concentration was reduced (S3), maintaining the parameters of Glenwood 2 (O'Brien and Julien, 1988), showed greater similarity to the original 2012 lahar deposit. However, at several points in the area, it significantly exceeds the recorded limits, and the maximum depth does not align with the PSI. Once these comparisons were

made, we considered that the parameters used for the definitive modelling of the 2012 lahar (OS) more accurately reproduce its spatial distribution; therefore, there is a better fit to the maximum flow depths. To demonstrate the above idea, Figure 9B shows a maximum difference in depths between simulations of up to 1.84 m.

Following the completion of the simulations, it was determined that the parameters proposed by O'Brien and Julien (1988) in Glenwood 2 reflected a better fit with the PSIs used as a calibrator for the models. These parameters were selected based on their ability to facilitate a flow that traversed the entire channel, maintain deposition consistent with observations made in the field, observations made through satellite imagery, and produce velocity values corresponding to the dimensions of the channel.

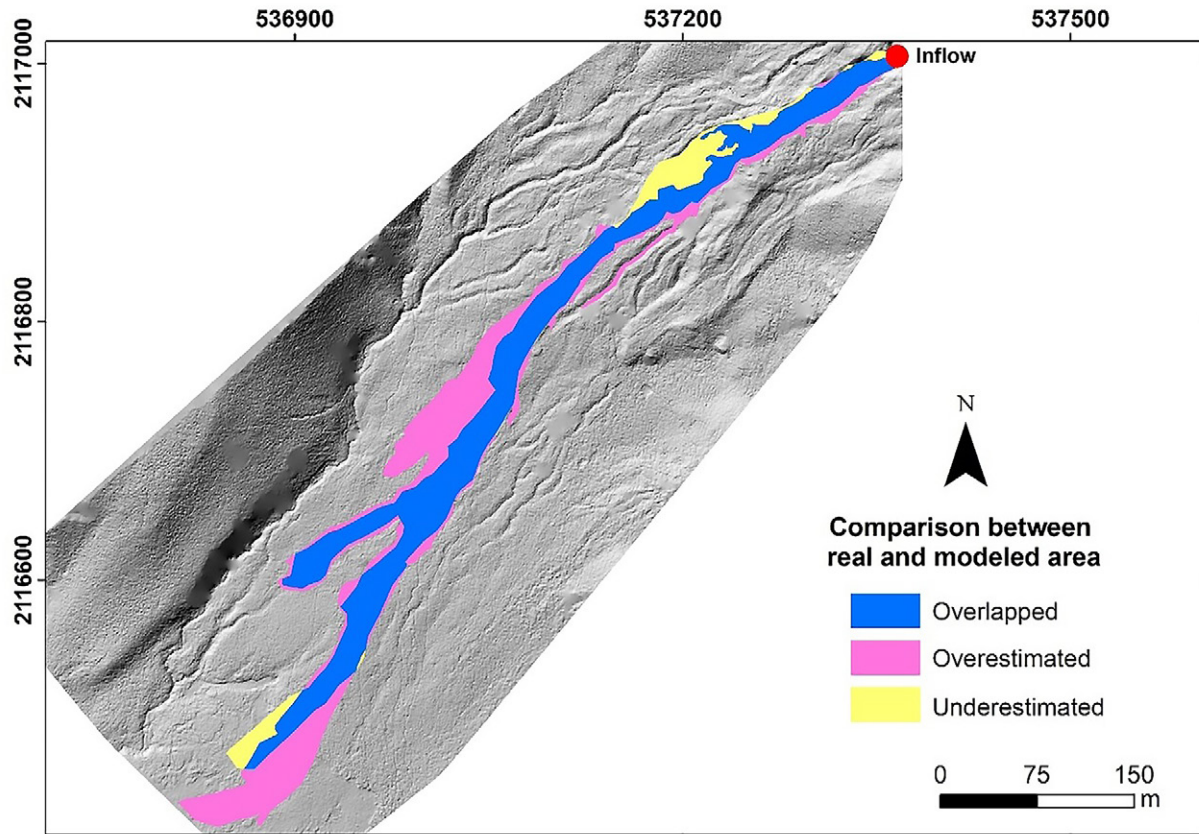


Figure 8 The validation of the lahar simulation was performed by comparing the actual inundated areas with those simulated by the HEC-RAS software (WGS 84/UTM zone 14N).

5. Discussion

5.1. SIGNIFICANCE OF GEOMORPHOLOGICAL MAPPING IN LAHAR MANAGEMENT

The geomorphological mapping of lahars is crucial for identifying potential routes and flooding areas. Consequently, a better understanding of their spatial distribution and recurrence enables more effective management, particularly in locations where their dynamics are not well understood. In other words, identifying each landform contributes to a comprehensive understanding of the processes occurring at these sites. In this context, the two maps of the Alcalican Valley presented in this research show the geomorphological dynamics of the area. Firstly, an analysis of the general context of the valley revealed that the constant supply of fragmented material from the highly fractured lavas, arranged as a colluvial ramp, is the primary source of lahars in the valley. The detailed map reinforces this concept by accurately delineating the 2012 lahar and identifying a sequence of ancient laharic lobes. This illustrates that, under specific conditions, laharic dynamics can be a recurrent phenomenon within the valley, despite its apparent stability.

It is also noteworthy that, although Alcalican Valley has been one of the most frequently visited

areas within the Iztaccihuatl-Popocatepetl National Park, there is currently no available geomorphological information. Consequently, creating a geomorphological map could be invaluable for a more effective management of this region.

5.2. ROLE OF DENDROGEOMORPHOLOGY AND BOTANICAL-BASED EVIDENCE IN LAHAR MODELLING

Regarding the dendrogeomorphological analysis, the *Pinus hartwegii* trees were found to be suitable for recording geomorphological processes in the Alcalican Valley. Other studies have demonstrated the effectiveness of this method in different volcanic areas of the TMVB, as shown by Bollschweiler *et al.* (2010), Franco-Ramos *et al.* (2016a, 2026b, 2017), Figueroa-García *et al.* (2021), and Vázquez-Ríos and Franco-Ramos (2022). For the lahar event dated in 2012 in the Alcalican valley, there is clear evidence that the flow triggers had a regional occurrence, as several lahars have been dated in other volcanic structures of the TMVB, such as Pico de Orizaba (Franco-Ramos *et al.*, 2020; Vázquez-Ríos and Franco-Ramos, 2022), La Malinche (Franco-Ramos *et al.*, 2017), and Popocatepetl (Franco-Ramos *et al.*, 2016a).

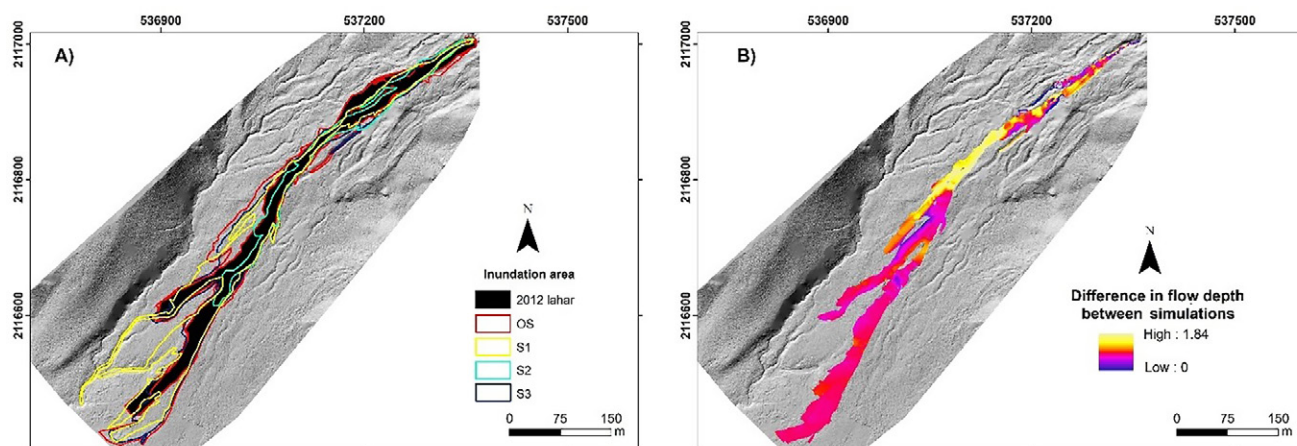


Figure 9 Simulation results using different rheological coefficients. A) Areas of inundation; B) Differences in flow depth (WGS 84/UTM zone 14N).

Using botanical-based evidence, such as PSIs (Benito and Thorndycraft, 2005; Baker, 2008; Ballesteros-Cánovas *et al.*, 2011; Díez-Herrero *et al.*, 2013) will help to validate the models and research outcomes, particularly in regions where alternative monitoring techniques, like rain gauges and geophones, are unavailable. The PSIs employed in this research showed a satisfactory fit with a peak discharge of 5 m³/s. The models exhibited a standard deviation of -0.26 m between the debarking and the flow depth, while the average fit for all the trees considered was 0.01 m. This adjustment largely reflects the geomorphological position of the trees, specifically those on terraces near the riverbed with one tree even situated inside the ravine. Consequently, the interaction between the trees and the flow was direct, and there is no evidence to suggest that the impact was caused by a block forcefully expelled due to the intensity of the lahar. Additionally, the results of the simulations were validated with parameters such as PLR, demonstrating a satisfactory correspondence between the simulated results and the actual lahar flow deposit.

5.3 ADVANCES AND CHALLENGES IN LAHAR MODELLING

The employment of numerical modelling was used to demonstrate its competence in accurately reconstructing the spatial distribution and magnitude (in terms of peak discharge) of the 2012 lahar in the Alcalican valley (central Mexico).

Lahars have been studied for several decades due to their impacts on people living in flood-prone areas (Lavigne and Suwa, 2004; Pelfini and Santilli, 2008; Capra *et al.*, 2018; Thouret *et al.*, 2020). One of the most significant challenges currently facing the field is the development of more accurate models capable of predicting the distribution of lahars and calculating flow depths in populated areas. This requires validation of the results produced by different models under varying geomorphological conditions using multiple techniques, such as PSIs, among others.

An illustrative example is the work conducted by Worni *et al.* (2012), who analyzed a lahar that occurred in 2007 at the Nevado de Huila (Colombia). They modelled the event using the software LAHARZ and FLO-2D, calibrating their models with hydrographs, seismic geophones, and fieldwork to assess its spatial distribution. Additionally, they created scenarios with varying volumes to determine the potential magnitudes that nearby populations might face.

Another key study on lahar analysis and modelling was conducted by Thouret *et al.* (2023), focusing on the Merapi volcano known for its high level of activity and frequent lahar formation. The FLO-2D model was employed to generate a series of scenarios aimed at refining the region's risk map.

With regard to the modelling of lahars in central Mexico, several studies have focused on the most significant volcanic structures, including the Popocatepetl volcano (Muñoz-Salinas *et al.*, 2009; Caballero and Capra, 2014; Zaragoza *et al.*, 2020), Colima volcano (Vázquez *et al.*, 2014; Caballero *et al.*, 2016), Pico de Orizaba volcano (Hubbard *et al.*, 2007; Franco-Ramos *et al.*, 2020; Figueroa-García *et al.*, 2021), Ceboruco volcano (Sieron *et al.*, 2019) and Tacaná volcano (Vázquez *et al.*, 2021). These studies utilized various software and models, such as FLO-2D (O'Brien *et al.*, 1993), RAMMS (Christen *et al.*, 2012) and LAHARZ (Schilling, 2014). It is important to note that research in Mexico has predominantly focused on active volcanoes.

Therefore, recognizing and analyzing intra-eruptive lahars (*i.e.*, phenomena that occur within the ravines of dormant or extinct volcanoes) is crucial. Such lahars are also prevalent throughout much of the TMVB. One example can be observed in the Alcalican valley of the Iztaccíhuatl volcano.

5.4. HEC-RAS SOFTWARE AND THE CRITICAL ROLE OF ACCURATE DEMS IN LAHAR MODELLING

The HEC-RAS open-source software demonstrates satisfactory performance in modelling lahar processes, with minimal discrepancies observed in various validation tests and a satisfactory

alignment with field observations. Its capacity to create detailed water surface profiles and predict sediment transport makes HEC-RAS well-suited for accurately modelling the complex behaviors of lahars, which include rapid flows of water and debris. This modelling capability is invaluable for understanding the potential impacts and behaviors of lahars across various scenarios (Satria *et al.*, 2024). Additionally, HEC-RAS facilitates multi-parameter analysis, incorporating variables such as flow velocity, depth, and sediment concentration. This capability allows for a more detailed characterization of lahar flows than models that primarily consider flow paths and extents (Jenkins *et al.*, 2015).

It is noteworthy that, in addition to being open-source software, it offers a wide range of equations for modelling non-Newtonian flows, allowing for the integration of different values of viscosity and stress. This capability is particularly useful for simulating various types of lahars and enables the performance of additional sensitivity tests, thereby reducing uncertainty. The corroboration of simulation results was achieved through the implementation of sensitivity tests on yield stress (α) and viscosity (β). These tests revealed significant variations in the area and depth of flow when the values proposed by O'Brien and Julien (1988) were modified. This evidence supports the assertion that HEC-RAS functions effectively when these values are introduced into its DebrisLib module (Gibson *et al.*, 2021; Gibson *et al.*, 2022). Nevertheless, it is important to note that numerical simulations inherently involve considerable uncertainty associated with input parameters, including sediment concentration and rheology. Therefore, a systematic evaluation of these parameters is essential before employing this type of tool.

Nevertheless, it is essential to acknowledge that the Digital Elevation Model (DEM) remains a pivotal component. It serves as an input that preserves as much terrain detail as possible, including terraces, the actual width of the main channel, and changes in the river's direction.

This information is crucial, as the software will consider these limits or obstacles during modelling, thereby reducing the likelihood of excessive overflows (Capra *et al.*, 2011). Furthermore, understanding the parameters and observations made in the field is critical for the deposit distribution.

One of the principal considerations in modelling lahars is the resolution and accuracy of the DEM. A 70x70 centimeter pixel DEM is employed to identify the various landforms within the channel. Vegetation was filtered out to accurately depict the terrain, ensuring consistency and accuracy in the simulation. However, it should be noted that the model used in this study is based on a DEM reflecting post-event morphology, which may introduce a certain margin of error. To minimize this potential error, eight cross-sectional profiles were generated along the main channel using a GNSS/GPS millimetric system and compared with those derived directly from the DEM (Figure 10). This approach allowed for the correction and verification that no deposits associated with the 2012 event (or any subsequent events) were present within the channel that could act as barriers and distort the modeling results.

5.5. VALIDATION OF THE 2012 LAHAR MODEL AND IDENTIFICATION OF ITS TRIGGERS

The results indicated that the application of PLR and e_1 equations validated the modelling of the 2012 flow within the Alcalican Valley with values of 107% and 0.72, respectively. These results demonstrate that it can be considered optimal, as the discrepancies between the model and reality are minimal. Similar values were obtained in other studies, such as the one presented by Charbonnier *et al.* (2018) for the Toliman volcano (Guatemala), where his PLR value was 103%. Similarly, Caballero *et al.* (2016) employed both methods to validate their modelling in the Montegrande Ravine (Colima Volcano), resulting in PLR values of 105% for PLR and e_1 values of 0.78. These three study cases provide compelling

evidence that calibrated modelling is an effective approach. The discrepancies between the observed reality and the modelled results may be attributed to several factors, including the constitutive equations employed by the HEC-RAS open-source software, which governs the deposition and erosion of materials in sectors where the channel undergoes a change in direction. Additionally, these outcomes may also be influenced by the current morphology of the valley. Although the maximum discharge assessed for the 2012 lahar can be considered low, several factors must be assessed for future scenarios. The first one relates to the fact that the Alcalican Valley maintains an active channel, particularly during the rainy season (June to October). The second factor concerns the availability of material for

mobilization, as the fractured lavas surrounding the upper portion of the valley continuously contribute debris to the slopes. In this sense, a review of the seismic record prior to these dates was carried out to verify if there was an anomalous contribution of material in the area, and it was found that on March 20th, 2012, there was an earthquake of magnitude 7.5 with epicenter in the city of Ometepec, Guerrero, 400 km away from the study area (SSN, 2024), so there is a probability that the material mobilized in the form of a lahar in August 2012 is related to this seismic event, however, more elements would be needed to confirm this fact.

It can be demonstrated that the sudden influx of material and precipitation led to the formation of a lahar on a relatively stable surface. This

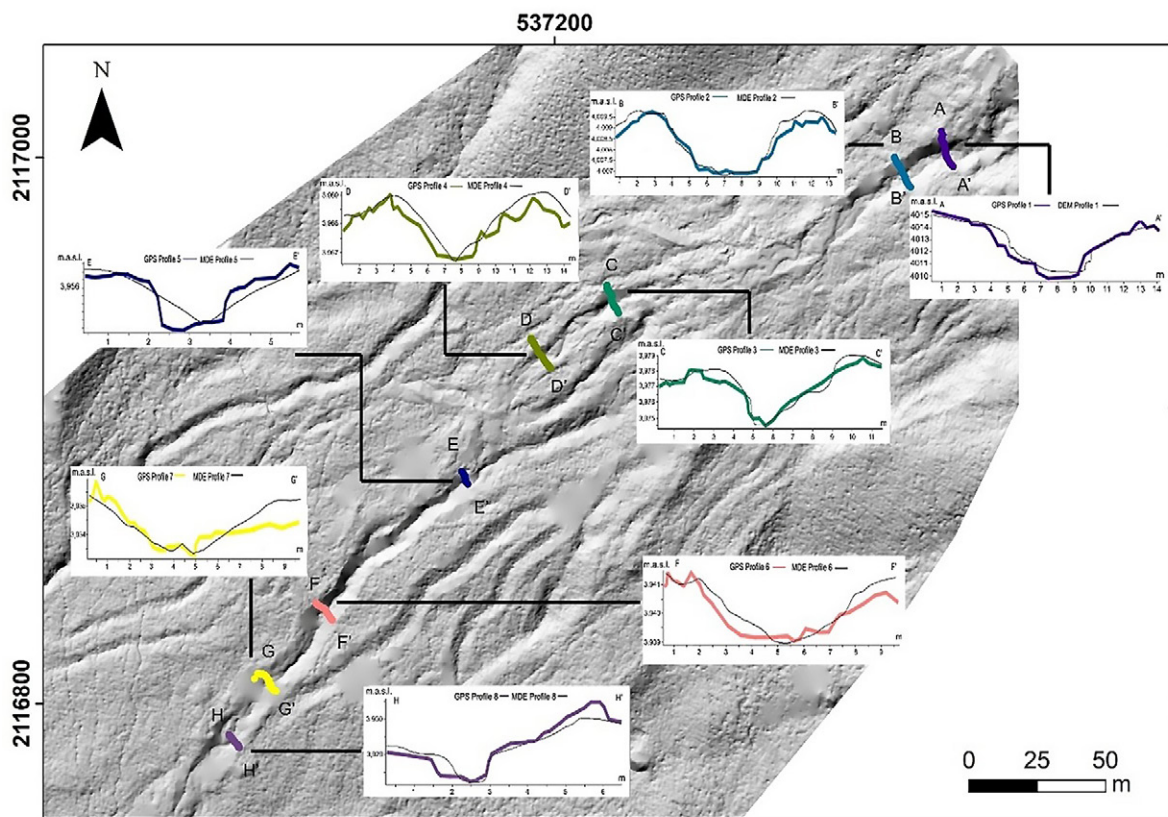


Figure 10 The map shows the eight profiles obtained using a millimetric GNSS/GPS system, along with a comparison to profiles obtained from DEMs, generated through drone flights. The purpose is to demonstrate that the model is accurate and does not present any obstacle that could modify the fluvial discharge simulated in HEC-RAS. The correspondence between the two sets of profiles is evident; however, in some instances, certain landforms (profile 4 and 5) are not captured, due to the resolution of the DEM. Nevertheless, the channel and its dimensions remain consistent (WGS 84/UTM zone 14N).

situation poses a greater risk, as the probability of lahar formation increases when these factors converge. This aspect is particularly important to consider, given that the area is frequently traversed by climbers and hikers. Similar processes have been documented by Dufresne and Geertsema (2020), who reported large rockslides in northern British Columbia between 2002 and 2005 that evolved into debris flows. Although these phenomena were of considerable magnitude, their genesis and development are comparable to those in our study area. Additional relevant study is that of Guo *et al.* (2021), which reported a gravitational process in southwest China in August 2020, generated by an active fault system that resulted in a debris flow due to heavy rainfall (315 mm over 24 days and 32 mm/day as the trigger rainfall of the event). Another clear example of similar dynamics is presented by Ballesteros-Cánovas *et al.* (2023) who explains the relationship between extreme rainfall and the occurrence of earthquakes as triggers of debris flows in the Japanese Alps.

In the case of Mexico, a study conducted by Zaragoza *et al.* (2020) provides a comparable example to the 2012 lahar in the Alcalican Valley regarding its genesis, dynamics, and geographical proximity. This study focuses on the lahars that occurred in 2010, within the Nexpayantla Ravine (Popocatepetl volcano). In this work, the researchers identified precipitation (100 mm/day) and the sudden contribution of material from sheet erosion and mass wasting processes as the triggering factors. This is analogous to the situation presented in this investigation. Although the previous references serve as potential bases for explaining the processes that occurred in the Alcalican Valley, it can also be suggested that the phenomenon was influenced by the morphology and dimensions of the watershed, which impacts the saturation of the fluvial system and increases the likelihood of these processes (Coussot and Meunier, 1996). Although it is possible to establish values for volume or average discharge under certain conditions, it is crucial to consider other factors that may influence the behavior and occurrence of lahars.

6. Conclusions

The present study validates the potential application of dendrogeomorphology, PSIs and the open-source software HEC-RAS, to assess the spatial distribution and magnitude of lahars in currently inactive volcanoes of central Mexico, which are primarily caused by hydrometeorological phenomena. HEC-RAS is considered a viable option due to its open-source nature and the numerous advantages it offers over other commonly used software. These advantages include the capacity to utilize different equations that account for the rheology of the flows, as well as the program's sensitivity to variations in viscosity and stress values, enabling a closer approximation to the physical conditions. The use of botanical PSIs for thickness calibration is a pivotal aspect, as it minimizes the uncertainty typically associated with calculating this value. However, it is essential to consider the presence and distribution of trees along the channel. In Alcalican Valley, the behavior of the lahar that occurred in 2012 is particularly noteworthy, as it allowed for the definition of its magnitude, triggers (including geologic-geomorphological factors, the rainy season and the influence of Hurricane Ernesto) and distribution. This study provides insights into the morpho-dynamics of lahars, thereby enhancing the understanding of these processes in high-mountain volcanic basins. It may also be useful for the management and planning of the Iztaccíhuatl-Popocatepetl National Park.

Contributions of authors

The authors contributed equally to the conceptualization, development, and execution of the lahar study presented here, including the analysis, preparation of figures and other graphic materials, as well as the writing and final preparation of the present manuscript.

Financing

This research was funded by DGAPA-PAPIIT, UNAM project numbers IN100522 and IN119620. Additional support to the first author (JEFG) is from a PhD Scholarship provided by CONAHCYT.

Acknowledgements

We kindly thank Omar Hernández Rivas and Marco Antonio Pablo Pablo for their assistance during fieldwork.

Conflicts of interest

The authors declare no conflicts of interest.

Handling editor

Adolfo Quesada Román.

References

- Andrés, N., Palacios, D., Zamorano, J.J., Vázquez-Selem, L., 2011, Shallow ground temperatures and periglacial processes on Iztaccíhuatl Volcano, Mexico: Permafrost and Periglacial Processes, 22(2), 188–194. <https://doi.org/10.1002/ppp.713>
- Arroyo-Solórzano, M., Quesada-Román, A., Barrantes-Castillo, G., 2022, Seismic and geomorphic assessment for coseismic landslides zonation in tropical volcanic contexts: Natural Hazards, 114(3), 2811–2837. <https://doi.org/10.1007/s11069-022-05492-8>
- Baker, V.R., 2008, Paleoflood hydrology: Origin, progress, prospects: Geomorphology, 101(1–2), 1–13. <https://doi.org/10.1016/j.geomorph.2008.05.016>
- Ballesteros-Cánovas, J.A., Eguibar, M., Bodoque, J.M., Díez-Herrero, A., Stoffel, M., Gutiérrez-Pérez, I., 2011, Estimating flash flood discharge in an ungauged mountain catchment with 2D hydraulic models and dendrogeomorphic palaeostage indicators: Hydrological Processes, 25(6), 970–979. <https://doi.org/10.1002/hyp.7888>
- Ballesteros-Cánovas, J.A., Czajka, B., Janecka, K., Lempa, M., Kaczka, R.J., Stoffel, M., 2015a, Flash floods in the Tatra Mountain streams: Frequency and triggers: Science of the Total Environment, 511, 639–648. <https://doi.org/10.1016/j.scitotenv.2014.12.081>
- Ballesteros-Cánovas, J.A., Márquez-Peñaranda, J.F., Sánchez-Silva, M., Díez-Herrero, A., Ruiz-Villanueva, V., Bodoque, J.M., Eguibar, M.A., Stoffel, M., 2015b, Can tree tilting be used for paleoflood discharge estimations?: Journal of Hydrology, 529(P2), 480–489. <https://doi.org/10.1016/j.jhydrol.2014.10.026>
- Ballesteros-Cánovas, J.A., Stoffel, M., Spyt, B., Janecka, K., Kaczka, R.J., Lempa, M., 2016, Paleoflood discharge reconstruction in Tatra Mountain streams: Geomorphology, 272, 92–101. <https://doi.org/10.1016/j.geomorph.2015.12.004>
- Ballesteros-Cánovas, J.A., Kariya, Y., Imaizumi, F., Manchado, A.M.T., Nishii, R., Matsuoka, N., Stoffel, M., 2023, Debris-flow activity in the Japanese Alps is controlled by extreme precipitation and ENSO – Evidence from multi-centennial tree-ring records: Global and Planetary Change, 231(May). <https://doi.org/10.1016/j.gloplacha.2023.104296>
- Baumann, V., Bonadonna, C., Cuomo, S., Moscariello, M., 2020, Modelling of erosion processes associated with rainfall-triggered lahars following the 2011 Cordon Caulle eruption (Chile): Journal of Volcanology and Geothermal Research, 390, 106727. <https://doi.org/10.1016/j.jvolgeores.2019.106727>
- Benito, G., Thorndycraft, V.R., 2005, Palaeoflood hydrology and its role in applied hydrological sciences: Journal of Hydrology, 313(1–2), 3–15. <https://doi.org/10.1016/j.jhydrol.2005.02.002>

- Bodoque, J.M., Eguibar, M.A., Díez-Herrero, A., Gutiérrez-Pérez, I., Ruiz-Villanueva, V., 2011, Can the discharge of a hyperconcentrated flow be estimated from paleoflood evidence?: *Water Resources Research*, 47(12), 1–14. <https://doi.org/10.1029/2011WR010380>
- Bodoque, J.M., Díez-Herrero, A., Eguibar, M.A., Benito, G., Ruiz-Villanueva, V., Ballesteros-Cánovas, J.A., 2015, Challenges in paleoflood hydrology applied to risk analysis in mountainous watersheds - A review: *Journal of Hydrology*, 529(P2), 449–467. <https://doi.org/10.1016/j.jhydrol.2014.12.004>
- Bollschweiler, M., Stoffel, M., Vázquez-Selem, L., Palacios, D., 2010, Tree-ring reconstruction of past lahar activity at Popocatepetl volcano, Mexico: *Holocene*, 20(2), 265–274. <https://doi.org/10.1177/0959683609350394>
- Bovi, R.C., Romanelli, J.P., Caneppele, B.F., Cooper, M., 2022, Global trends in dendrogeomorphology: A bibliometric assessment of research outputs: *Catena*, 210, 105921. <https://doi.org/10.1016/j.catena.2021.105921>
- Boyd, J., Chambers, J., Wilkinson, P., Peppas, M., Watlet, A., Kirkham, M., Jones, L., Swift, R., Meldrum, P., Uhlemann, S., Binley, A., 2021, A linked geomorphological and geophysical modelling methodology applied to an active landslide: *Landslides*, 18(8), 2689–2704. <https://doi.org/10.1007/s10346-021-01666-w>
- Brunner, G.W., 2002, Hec-ras (river analysis system): North American Water and Environment Congress and Destructive Water, ASCE, 3782–3787.
- Brunner, M.I., Slater, L., Tallaksen, L.M., Clark, M., 2021, Challenges in modeling and predicting floods and droughts: A review: *Wiley Interdisciplinary Reviews: Water*, 8(3), 1–32. <https://doi.org/10.1002/wat2.1520>
- Bühler, Y., Christen, M., Kowalski, J., Bartelt, P., 2011, Sensitivity of snow avalanche simulations to digital elevation model quality and resolution: *Annals of Glaciology*, 52(58), 72–80. <https://doi.org/10.3189/172756411797252121>
- Caballero, L., Capra, L., 2014, The use of FLO2D numerical code in lahar hazard evaluation at Popocatepetl volcano: A 2001 lahar scenario: *Natural Hazards and Earth System Sciences*, 14(12), 3345–3355. <https://doi.org/10.5194/nhess-14-3345-2014>
- Caballero, L., Capra, L., Vázquez, R., 2016, Evaluating the Performance of FLO2D for Simulating Past Lahar Events at the Most Active Mexican Volcanoes: Popocatepetl and Volcán de Colima. *Natural Hazard Uncertainty Assessment: Modeling and Decision Support*, 179–189. <https://doi.org/10.1002/9781119028116.ch12>
- Capra, L., Manea, V.C., Manea, M., Norini, G., 2011, The importance of digital elevation model resolution on granular flow simulations: A test case for Colima volcano using TITAN2D computational routine: *Natural Hazards*, 59(2), 665–680. <https://doi.org/10.1007/s11069-011-9788-6>
- Capra, L., Coviello, V., Borselli, L., Márquez-Ramírez, V.H., Arámbula-Mendoza, R., 2018, Hydrological control of large hurricane-induced lahars: Evidence from rainfall-runoff modeling, seismic and video monitoring: *Natural Hazards and Earth System Sciences*, 18(3), 781–794. <https://doi.org/10.5194/nhess-18-781-2018>
- Castruccio, A., Clavero, J., 2015, Lahar simulation at active volcanoes of the Southern Andes: implications for hazard assessment: *Natural Hazards*, 77(2), 693–716. <https://doi.org/10.1007/s11069-015-1617-x>
- Charbonnier, S.J., Connor, C.B., Connor, L.J., Sheridan, M.F., Oliva Hernández, J.P., Richardson, J.A., 2018, Modeling the October 2005 lahars at Panabaj (Guatemala): *Bulletin of Volcanology*, 80(1). <https://doi.org/10.1007/s00445-017-1169-x>
- Christen, M., Bühler, Y., Bartelt, P., Leine, R., Glover, J., Schweizer, A., Graf, C., Mcardell, B. W., Gerber, W., Deubelbeiss, Y., Feistl, T.,

- 2012, Integral Hazard Management Using a Unified Software Environment Numerical Simulation Tool “RAMMS”, in Congress Interpraevent, 77–86.
- Comisión Nacional de Áreas Naturales Protegidas (CONANP), 2013, Programa de manejo Parque Nacional Iztaccíhuatl-Popocatepetl, 26–40.
- Coussot, P., Meunier, M., 1996, Recognition, classification and mechanical description of debris flows: *Earth-Science Reviews*, 40(3–4), 209–227. [https://doi.org/10.1016/0012-8252\(95\)00065-8](https://doi.org/10.1016/0012-8252(95)00065-8)
- Coviello, V., Capra, L., Norini, G., Dávila, N., Ferrés, D., Márquez-Ramírez, V.H., Pico, E., 2021, Earthquake-induced debris flows at Popocatepetl Volcano, Mexico: *Earth Surface Dynamics*, 9(3), 393–412. <https://doi.org/10.5194/esurf-9-393-2021>
- De La Peña Guillén, K.A., Mendoza, M.E., Carlon Allende, T., Macías, J.L., Villanueva Díaz, J., 2025, Dendrogeomorphological analysis of a debris flow in the Monarch Butterfly Biosphere Reserve, central Mexico: *Natural Hazards*, 121(2), 1575–1598. <https://doi.org/10.1007/s11069-024-06873-x>
- Delgado-Granados, H., Miranda, P.J., Núñez, G.C., Pulgarín, B.A., Mothes, P., Roa, H.M., Cáceres Correa, B.E., Ramos, J.C., 2015, Hazards at Ice-Clad Volcanoes: Phenomena, Processes, and Examples From Mexico, Colombia, Ecuador, and Chile, in Shroder, J.F., Haerberli, W., Whiteman, C. (eds.), *Snow and Ice-Related Hazards, Risks, and Disasters*: Academic Press, 607–646. <https://doi.org/10.1016/B978-0-12-394849-6.00017-2>
- Díez-Herrero, A., Ballesteros-Cánovas, J.A., Bodoque, J.M., Ruiz-Villanueva, V., 2013, A new methodological protocol for the use of dendrogeomorphological data in flood risk analysis: *Hydrology Research*, 44(2), 234–247. <https://doi.org/10.2166/nh.2012.154>
- Díez-Herrero, A., Ballesteros, J.A., Ruiz-Villanueva, V., Bodoque, J.M., 2013, A review of dendrogeomorphological research applied to flood risk analysis in Spain: *Geomorphology*, 196, 211–220. <https://doi.org/10.1016/j.geomorph.2012.11.028>
- Dufresne, A., Geertsema, M., 2020, Rock slide–debris avalanches: flow transformation and hummock formation, examples from British Columbia: *Landslides*, 17(1), 15–32. <https://doi.org/10.1007/s10346-019-01280-x>
- Figueroa-García, J.E., Franco-Ramos, O., Bodoque, J.M., Ballesteros-Cánovas, J.A., Vázquez-Selem, L., 2021, Long-term lahar reconstruction in Jamapa Gorge, Pico de Orizaba (Mexico) based on botanical evidence and numerical modelling: *Landslides*, March. <https://doi.org/10.1007/s10346-021-01716-3>
- Franco-Ramos, O., Stoffel, M., Vázquez-Selem, L., Capra, L., 2013, Spatio-temporal reconstruction of lahars on the southern slopes of Colima volcano, Mexico – A dendrogeomorphic approach: *Journal of Volcanology and Geothermal Research*, 267, 30–38. <https://doi.org/10.1016/j.jvolgeores.2013.09.011>
- Franco-Ramos, O., Castillo, M., Muñoz-Salinas, E., 2016a, Using tree-ring analysis to evaluate intra-eruptive lahar activity in the Nexpayantla Gorge, Popocatepetl volcano (central Mexico): *Catena*, 147, 205–215. <https://doi.org/10.1016/j.catena.2016.06.045>
- Franco-Ramos, O., Stoffel, M., Vázquez-Selem, L., 2016b, Tree-ring based record of intra-eruptive lahar activity: Axaltzintle valley, Malinche volcano, Mexico: *Geochronometria*, 43(1), 74–83. <https://doi.org/10.1515/geochr-2015-0033>
- Franco-Ramos, O., Stoffel, M., Vázquez-Selem, L., 2017, Tree-ring based reconstruction of rockfalls at Cofre de Perote volcano, Mexico: *Geomorphology*, 290, 142–152. <https://doi.org/10.1016/j.geomorph.2017.04.003>
- Franco-Ramos, O., Ballesteros-Cánovas, J.A., Figueroa-García, J.E., Vázquez-Selem, L.,

- Stoffel, M., Caballero, L., 2020, Modelling the 2012 Lahar in a Sector of Jamapa Gorge (Pico de Orizaba Volcano, Mexico) Using RAMMS and Tree-Ring Evidence: *Water*, 12(2), 333. <https://doi.org/10.3390/w12020333>
- Frimberger, T., Andrade, S.D., Weber, S., Krautblatter, M., 2021, Modelling future lahars controlled by different volcanic eruption scenarios at Cotopaxi (Ecuador) calibrated with the massively destructive 1877 lahar: *Earth Surface Processes and Landforms*, 46(3), 680–700. <https://doi.org/10.1002/esp.5056>
- Gibson, S., Floyd, I., Sánchez, A., Heath, R., 2021, Comparing single-phase, non-Newtonian approaches with experimental results: Validating flume-scale mud and debris flow in HEC-RAS: *Earth Surface Processes and Landforms*, 46(3), 540–553. <https://doi.org/10.1002/esp.5044>
- Gibson, S., Moura, L.Z., Ackerman, C., Ortman, N., Amorim, R., Floyd, I., Eom, M., Creech, C., Sánchez, A., 2022, Prototype Scale Evaluation of Non-Newtonian Algorithms in HEC-RAS: Mud and Debris Flow Case Studies of Santa Barbara and Brumadinho: *Geosciences*, 12(3), 134. <https://doi.org/10.3390/geosciences12030134>
- Guo, J., Wang, J., Li, Y., Yi, S., 2021, Discussions on the transformation conditions of Wangcang landslide-induced debris flow: *Landslides*, 18(5), 1833–1843. <https://doi.org/10.1007/s10346-021-01650-4>
- Hubbard, B.E., Sheridan, M.F., Carrasco-Núñez, G., Díaz-Castellón, R., Rodríguez, S.R., 2007, Comparative lahar hazard mapping at Volcan Citlaltépetl, Mexico using SRTM, ASTER and DTED-1 digital topographic data: *Journal of Volcanology and Geothermal Research*, 160(1–2), 99–124. <https://doi.org/10.1016/j.jvolgeores.2006.09.005>
- Iverson, R.M., Reid, M.E., Logan, M., LaHusen, R.G., Godt, J.W., Griswold, J.P., 2011, Positive feedback and momentum growth during debris-flow entrainment of wet bed sediment: *Nature Geoscience*, 4(2), 116–121. <https://doi.org/10.1038/ngeo1040>
- Jenkins, S.F., Phillips, J.C., Price, R., Feloy, K., Baxter, P.J., Hadmoko, D.S., de Bézizal, E., 2015, Developing building-damage scales for lahars: application to Merapi volcano, Indonesia: *Bulletin of Volcanology*, 77(9). <https://doi.org/10.1007/s00445-015-0961-8>
- Lavigne, F., Suwa, H., 2004, Contrasts between debris flows, hyperconcentrated flows and stream flows at a channel of Mount Semeru, East Java, Indonesia: *Geomorphology*, 61(1–2), 41–58. <https://doi.org/10.1016/j.geomorph.2003.11.005>
- López-López, A.B., Vázquez-Selem, L., Siebe, C., Cruz-Flores, G., Correa-Metrio, A., 2023, Effect of elevation and slope orientation on pedogenesis of late Holocene volcanic ash on a tropical high mountain in central Mexico: *Catena*, 231(June). <https://doi.org/10.1016/j.catena.2023.107288>
- Macías, J.L., Arce, J.L., García-Tenorio, F., Layer, P.W., Rueda, H., Reyes-Agustin, G., López-Pizaña, F., Avellán, D., 2012, Geology and geochronology of Tlaloc, Telapón, Iztaccíhuatl, and Popocatepetl volcanoes, Sierra Nevada, central Mexico. In Aranda-Gómez, J.J., Tolson, G., Molina-Garza, R. S. (eds.), *The Southern Cordillera and Beyond: Geological Society of America, GSA Field Guides*, 25 3381–3392. [https://doi.org/10.1130/2012.0025\(08\)](https://doi.org/10.1130/2012.0025(08))
- Manville, V., Németh, K., Kano, K., 2009, Source to sink: A review of three decades of progress in the understanding of volcanoclastic processes, deposits, and hazards: *Sedimentary Geology*, 220(3–4), 136–161. <https://doi.org/10.1016/j.sedgeo.2009.04.022>
- Muñoz-Salinas, E., Castillo-Rodríguez, M., Manea, V., Manea, M., Palacios, D., 2009, Lahar flow simulations using LAHARZ program: Application for the Popocatepetl volcano, Mexico: *Journal of*

- Volcanology and Geothermal Research, 182(1–2), 13–22. <https://doi.org/10.1016/j.jvolgeores.2009.01.030>
- National Oceanic and Atmospheric Administration (NOAA), 2019, Historical Hurricanes Tracks (online): National Oceanic and Atmospheric Administration, last modified the 11th of March 2025, available <<https://coast.noaa.gov/hurricanes/>>, accessed November 17, 2025.
- Nixon, G.T., 1989, The geology of Iztaccíhuatl volcano and adjacent areas of the Sierra Nevada and Valley of Mexico: Geological Society of America, Special Paper, 219. <https://doi.org/10.1130/SPE219-p1>
- O'Brien, J.S., Julien, P.Y., 1988, Laboratory analysis of mudflow properties: *Journal of Hydraulic Engineering*, 114(8), 877–887.
- O'Brien, J.S., Julien, P.Y., Fullerton, W.T., 1993, Two-Dimensional Water Flood and Mudflow Simulation: *Journal of Hydraulic Engineering*, 119(2), 244–261. [https://doi.org/10.1061/\(ASCE\)0733-9429\(1993\)119:2\(244\)](https://doi.org/10.1061/(ASCE)0733-9429(1993)119:2(244))
- Pandey, V.K., Kumar, R., Singh, R., Kumar, R., Rai, S.C., Singh, R.P., Tripathi, A.K., Soni, V.K., Ali, S.N., Tamang, D., Latief, S.U., 2022, Catastrophic ice-debris flow in the Rishiganga River, Chamoli, Uttarakhand (India): *Geomatics, Natural Hazards and Risk*, 13(1), 289–309. <https://doi.org/10.1080/19475705.2021.2023661>
- Pelfini, M., Santilli, M., 2008, Frequency of debris flows and their relation with precipitation: A case study in the Central Alps, Italy: *Geomorphology*, 101(4), 721–730. <https://doi.org/10.1016/j.geomorph.2008.04.002>
- Pierson, T.C., Wood, N.J., Driedger, C.L., 2014, Reducing risk from lahar hazards: Concepts, case studies, and roles for scientists: *Journal of Applied Volcanology*, 3(1), 1–25. <https://doi.org/10.1186/s13617-014-0016-4>
- Pistolesi, M., Cioni, R., Rosi, M., Aguilera, E., 2014, Lahar hazard assessment in the southern drainage system of Cotopaxi volcano, Ecuador: Results from multiscale lahar simulations: *Geomorphology*, 207, 51–63. <https://doi.org/10.1016/j.geomorph.2013.10.026>
- Procter, J., Zernack, A., Mead, S., Morgan, M., Cronin, S., 2021, A review of lahars; past deposits, historic events and present-day simulations from Mt. Ruapehu and Mt. Taranaki, New Zealand: *New Zealand Journal of Geology and Geophysics*, 64(2–3), 479–503. <https://doi.org/10.1080/00288306.2020.1824999>
- Proietti, C., Coltelli, M., Marsella, M., Fujita, E., 2009, A quantitative approach for evaluating lava flow simulation reliability: LavaSIM code applied to the 2001 Etna eruption: *Geochemistry, Geophysics, Geosystems*, 10(9), 1–17. <https://doi.org/10.1029/2009GC002426>
- Quesada-Román, A., Fallas-López, B., Hernández-Espinoza, K., Stoffel, M., Ballesteros-Cánovas, J.A., 2019, Relationships between earthquakes, hurricanes, and landslides in Costa Rica: *Landslides*, 16, 1539–1550. <https://doi.org/10.1007/s10346-019-01209-4>
- Quesada-Román, A., Ballesteros-Cánovas, J.A., George, S.S., Stoffel, M., 2022, Tropical and subtropical dendrochronology: Approaches, applications, and prospects: *Ecological Indicators*, 144, 109506. <https://doi.org/10.1016/j.ecolind.2022.109506>
- Quesada-Roman, A., 2023, Dendrogeomorphology as a tool to depict hydrogeomorphic processes in the tropics: *Revista cartográfica*, (106), 35–51. <https://doi.org/10.35424/rcarto.i106.2120>
- Quesada-Román, A., 2024, Geomorphological effects of tropical cyclones in Costa Rica, Central America, in Coronato, A., Alves, G. B. (eds.), *Latin American Geomorphology: From the Crust to Mars*: Springer International Publishing, 101–116. https://doi.org/10.1007/978-3-031-55178-9_6
- Ruiz-Villanueva, V., Díez-Herrero, A., Stoffel, M., Bollschweiler, M., Bodoque, J.M.,

- Ballesteros, J.A., 2010, Dendrogeomorphic analysis of flash floods in a small ungauged mountain catchment (Central Spain): *Geomorphology*, 118(3–4), 383–392. <https://doi.org/10.1016/j.geomorph.2010.02.006>
- Salaorni, E., Stoffel, M., Tutubalina, O., Chernomorets, S., Seynova, I., Sorg, A., 2017, Dendrogeomorphic reconstruction of lahar activity and triggers: Shiveluch volcano, Kamchatka Peninsula, Russia: *Bulletin of Volcanology*, 79(1). <https://doi.org/10.1007/s00445-016-1094-4>
- Satria, H., Nurfaida, W., Kurniawan, A., Iswardoyo, J., Sulaiman, M., 2024, Numerical simulation and redesign of Kamar Kajang Levee against Mount Semeru lahar flood based on HEC-RAS 2D non-newtonian flow model: *IOP Conference Series: Earth and Environmental Science*, 1311(1). <https://doi.org/10.1088/1755-1315/1311/1/012065>
- Saucedo, R., Macías, J.L., Sarocchi, D., Bursik, M., Rupp, B., 2008, The rain-triggered Atenuique volcanoclastic debris flow of October 16, 1955 at Nevado de Colima Volcano, Mexico: *Journal of Volcanology and Geothermal Research*, 173(1–2), 69–83. <https://doi.org/10.1016/j.jvolgeores.2007.12.045>
- Schilling, S., 2014, Laharz _ py : GIS Tools for Automated Mapping of Lahar Inundation Hazard Zones: Reston, VA, Geological Survey, Open-File Report 2014-1073, 78 p. <https://doi.org/10.3133/ofr20141073>
- Schraml, K., Thomschitz, B., Mcardell, B.W., Graf, C., Kaitna, R., 2015, Modeling debris-flow runout patterns on two alpine fans with different dynamic simulation models: *Natural Hazards and Earth System Sciences*, 15(7), 1483–1492. <https://doi.org/10.5194/nhess-15-1483-2015>
- Servicio Sismológico Nacional (SSN), 2024, Reporte de actividad sísmica: Instituto de Geofísica, UNAM, disponible en <<https://www.ssn.unam.mx>>, consultado el 17 noviembre de 2025.
- Sieron, K., Ferrés, D., Siebe, C., Constantinescu, R., Capra, L., Connor, C., Connor, L., Groppelli, G., González Zuccolotto, K., 2019, Ceboruco hazard map: part II—modeling volcanic phenomena and construction of the general hazard map.: *Natural Hazards*, 96(2), <https://doi.org/10.1007/s11069-019-03577-5>
- Spataro, W., D'Ambrosio, D., Rongo, R., Trunfio, G.A., 2004, An evolutionary approach for modelling lava flows through cellular automata (Lecture Notes) in 6th International Conference on Cellular Automata for Research and Industry, 2004 October 25–28: Amsterdam, The Netherlands, Springer Berlin, Heidelberg, 3305, 725–734. https://doi.org/10.1007/978-3-540-30479-1_75
- Stoffel, M., Corona, C., 2014, Dendroecological Dating of Geomorphic Disturbance in Trees: *Tree-Ring Research*, 70(1), 3–20. <https://doi.org/10.3959/1536-1098-70.1.3>
- Sunyé-Puchol, I., Hodgetts, A.G.E., Watt, S.F.L., Arce, J.L., Barfod, D.N., Mark, D.F., Sosa-Ceballos, G., Siebe, C., Dymock, R.C., Blaauw, M., Smith, V.C., 2022, Reconstructing the middle to late Pleistocene explosive eruption histories of Popocatepetl, Iztaccíhuatl and Tláloc-Telapón volcanoes in Central México: *Journal of Volcanology and Geothermal Research*, 421. <https://doi.org/10.1016/j.jvolgeores.2021.107413>
- Tayyebi, S.M., Pastor, M., Hernandez, A., Gao, L., Stickle, M.M., Yifru, A.L., Thakur, V., 2022, Two-Phase Two-Layer Depth-Integrated SPH-FD Model: Application to Lahars and Debris Flows: *Land*, 11(10), 1–21. <https://doi.org/10.3390/land11101629>
- Thouret, J.C., Antoine, S., Magill, C., Ollier, C., 2020, Lahars and debris flows: Characteristics and impacts: *Earth-Science Reviews*, 201(November 2019). <https://doi.org/10.1016/j.earscirev.2019.103003>
- Thouret, J.C., Aisyah, N., Jenkins, S.F., de Bézizal, E., Sulistiyani, Charbonnier, S.J., Solikhin, A., 2023, Merapi's lahars: characteristics, behaviour, monitoring, impact, hazard

- modelling and risk assessment, in Gertisser, R., Troll, V.R., Walter, T.R., Agung Nandaka, I.G.M., Ratdompurbo, A. (eds.), Merapi Volcano: Geology, Eruptive Activity, and Monitoring of a High-Risk Volcano: Springer Cham, 553–572. https://doi.org/10.1007/978-3-031-15040-1_18
- Tichavský, R., 2023, Earth-Science Reviews Understanding hydrometeorological triggers of natural hazards through dendrogeomorphology : Methods, limitations, and challenges: Earth-Science Reviews, 244(August), 104546. <https://doi.org/10.1016/j.earscirev.2023.104546>
- Vázquez-Ríos, M., Franco-Ramos, O., 2022, Reconstrucción dendrogeomorfológica de procesos de remoción en masa y lahares en las Barrancas Seca y Ojo Salado, Pico de Orizaba, México: Investigaciones Geográficas, 107. <https://doi.org/10.14350/rig.60470>
- Vázquez-Selem, L., Heine, K., 2011, Late Quaternary Glaciation in Mexico: Developments in Quaternary Science, 15, 849–861. <https://doi.org/10.1016/B978-0-444-53447-7.00061-1>
- Vázquez, R., Capra, L., Caballero, L., Arámbula-Mendoza, R., Reyes-Dávila, G., 2014, The anatomy of a lahar: Deciphering the 15th September 2012 lahar at Volcán de Colima, Mexico: Journal of Volcanology and Geothermal Research, 272(September 2012), 126–136. <https://doi.org/10.1016/j.jvolgeores.2013.11.013>
- Vázquez, R., Macías, J.L., Arce, J.L., 2021, Integrated hazards maps of the Tacaná Volcanic complex, Mexico-Guatemala: Ashfall, block-and-ash flows, and lahars: Journal of South American Earth Sciences, 107(April 2020). <https://doi.org/10.1016/j.jsames.2020.103146>
- Wilford, D.J., Sakals, M.E., Grainger, W.W., Millard, T.H., Giles, T.R., 2009, Managing forested watersheds for hydrogeomorphic risks on fans. Bulletin: Land Management Handbook - Ministry of Forests and Range, 61, vi-62.
- Williams, R., Stinton, A.J., Sheridan, M.F., 2008, Evaluation of the Titan2D two-phase flow model using an actual event: Case study of the 2005 Vazcún Valley Lahar: Journal of Volcanology and Geothermal Research, 177(4), 760–766. <https://doi.org/10.1016/j.jvolgeores.2008.01.045>
- Wohl, E., Scott, D.N., 2017, Wood and sediment storage and dynamics in river corridors: Earth Surface Processes and Landforms, 42(1), 5–23. <https://doi.org/10.1002/esp.3909>
- Worni, R., Huggel, C., Stoffel, M., Pulgarín, B., 2012, Challenges of modeling current very large lahars at Nevado del Huila Volcano, Colombia: Bulletin of Volcanology, 74(2), 309–324. <https://doi.org/10.1007/s00445-011-0522-8>
- Yilmaz, K., Dinçer, A.E., Kalpakçı, V., Öztürk, Ş., 2023, Debris flow modelling and hazard assessment for a glacier area: a case study in Barsem, Tajikistan: Natural Hazards, 115(3), 2577–2601. <https://doi.org/10.1007/s11069-022-05654-8>
- Zaragoza, G., Caballero-García, L., Capra, L., Nieto-Torres, A., 2020, Lahares secundarios en el volcán Popocatepetl: El lahar Nexpayantla del 4 de febrero, 2010: Revista Mexicana de Ciencias Geológicas, 37(2), 121–134. <https://doi.org/10.22201/CGEO.20072902E.2020.2.1565>